----- CONFIDENTIAL -----

End of Year 1 Report, 29th July 2016

New Materials for Combatting and Understanding Infection

Laura Wilkins:

l.e.wilkins@warwick.ac.uk

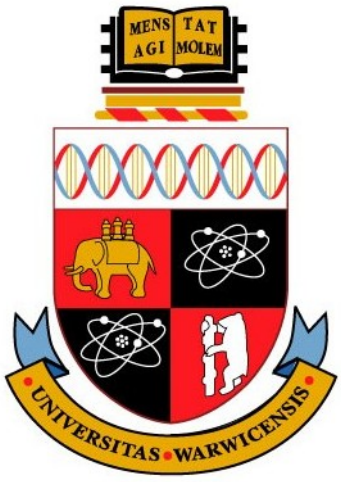

Supervisor: Prof. Matthew I. Gibson

Advisory Panel: Prof. Tim Bugg and Dr. Manuela Tosin

The Leverhulme Trust

Funded by The Leverhulme Trust

1 Abstract

Glycan-lectin interactions are central to many cell-surface interactions, such as the recognition and binding of bacterial toxin proteins. The use of multivalent polymers with saccharides attached at multiple sites along the chain exploits the cluster glycoside effect to enhance lectin affinity in anti-adhesion therapies. A key target for multivalent anti-adhesion therapy is CTx, the toxin secreted by Cholera that adheres to the human epithelial cell surface prior to Cholera infection. CTx has high affinity for GM1, a human glycolipid with a chain-end galactose residue and a side-branching sialic acid residue. Previous polymer mimics of this ligand have incorporated galactose functionality, though the inclusion of a second, side-branching moiety could further enhance binding.

In this study, GM1-mimics were generated through post-polymerisation modification of RAFT polymers. A thiolactone moiety was incorporated in these polymers through the RAFT copolymerisation of *N*-hydroxyethyl acrylamide with *N*-thiolactone acrylamide (5, 10, 20 and 100 molar %) to give polymers of narrow dispersity. The thiolactone moiety was opened by treatment with either benzylamine or glucosamine to liberate a thiol, which was then modified by radical-initiated Michael addition of allyl galactose. These modifications were confirmed by a representative sample characterised by NMR and DMF-SEC.

SwissDock modelling was performed on the modified repeat units to test if binding to the CTx active site was feasible. The *in vitro* inhibitory ability of the library of polymers against CTx was assessed with fluorescence-linked binding assays. The glucosamine/allyl galactose polymers displayed potent inhibitory activity, with lower molar percentages of thiolactone displaying the greater affinity. The 100% *N*-thiolactone acrylamide polymers did not show inhibitory activity, however. Further processing is required to take into account sugar concentration, and to calculate true IC_{50} values.

An additional investigation into protein-polymer conjugates was also begun. Benzylguanine (BG) is a versatile end group that interacts with SNAP-tagged proteins. In this investigation, BG-functionalised polymers were synthesized by chain-end displacement of a pentafluorophenol group incorporated in the RAFT chain transfer agent. These polymers were successfully conjugated to gold nanoparticles through their thiol end groups. Further work is required to assess ability to conjugate with SNAP-tag.

2 List of Tables and Figures

Figure 1: Adhesion and Anti-adhesion interactions of toxin such as CTx. 6

Figure 2: GM1 ligand binding to CTx protein. 8

Figure 3: Scheme of RAFT Polymerisation technique. 9

Figure 4: Common strategies used in post-polymerisation, partially adapted from reference 39. 10

Figure 5: Structure of GM1-ganglioside, and "ideal" doubly-modified polymer. 11

Figure 6: Synthesis of allyl and amino-sugars. 12

Figure 7: Transmission electron micrographs of PVC products from Reference 64. 13

Figure 8: Conjugation of modified polymers to proteins via AuNPs and SNAP-tag. 13

Figure 9: Scheme for synthesis of doubly modified GM1 mimic. 16

Table 1: Characterisation data of PFP- and BG-pHEAs. 17

Figure 10: Scheme for synthesis allyl and amino galactose sugars. 17

Table 2: SEC Data for modified pTLa. 18

Figure 11: Scheme for synthesis of benzylamine/glucosamine and allyl galactose-modified polymers. 18

Figure 12: Swiss-Dock binding outputs for glucosamine/allyl galactose and benzylamine/allyl galactose. 19

Figure 13: Fluorescence-linked sorbent assays to assess inhibitory activity of modified polymers. 20

Figure 14: Fluorescence-linked CTx-FITC binding curves for the polymers modified with glucosamine. 21

Figure 15: Fluorescence-linked CTx-FITC binding curves for the polymers modified with benzylamine. 21

Figure 16: Scheme for synthesis of AuNP-protein conjugate. 22

Table 3: Characterisation data of PFP- and BG-pHEAs. 22

Figure 17: DLS characterisation of polymer-conjugated AuNPs. 23

Table of Contents

1 Abstract **2**

2 List of Tables and Figures **3**

Table of Contents **4**

3 Introduction **6**

3.1 Glycans and Anti-Adhesion Therapy **6**

3.2 Reversible Addition- Fragmentation Atom Transfer Polymerisation for Controlled Glycopolymer Structure **8**

3.3 Modifiable *N*-Thiolactone Acrylamide Polymers **10**

3.4 Gold Nanoparticles as a Scaffold for Protein-Polymer Conjugates **12**

4 Aims **15**

5 Objectives **15**

6 Milestones for year 1 ..... **15**

7 Results and Discussion **16**

7.1 Synthesis of Doubly-Modified Polymers **16**

7.2 Inhibitory activity of Doubly-modified Polymers **19**

7.3 Synthesis of SNAP-tag-able Gold Nanoparticles **21**

7.4 Conclusions **23**

8 Future work **25**

9 Materials and Methods **26**

9.1 Materials **26**

9.2 Analytical Methods **26**

9.3 Synthetic Methods **27**

9.3.1 Synthesis of 2-(dodecylthiocarbonothioylthio)-2-methylpropionic acid (DMP/DDMAT) 27

9.3.2 Synthesis of *N*-Thiolactone Acrylamide 27

9.3.3 Synthesis of b-D-galactose pentaacetate 28

9.3.4 Synthesis of 1-b-allyl-D-galactose 29

9.3.5 Synthesis of 1-amino-b-D-galactosamine 30

9.3.6 (Unsuccessful) Synthesis of Amino-Sialic Acid 31

9.3.7 General Procedure for Polymerisation of *N*-hydroxyethyl acrylamide (HEA) 31

9.3.8 General Procedure for Polymerisation of *N*-isopropyl acrylamide (NIPAM) 32

9.3.9 General Procedure for Copolymerisation of *N*-hydroxyethyl acrylamide (HEA) and *N*-thiolactone acrylamide (TLa) 33
9.3.10 (Unsuccessful) General Procedure for Copolymerisation of *N*-isopropyl acrylamide (NIPAM) and *N*-thiolactone acrylamide (TLa) 34
9.3.11 General Procedure for Polymerisation of *N*-thiolactone acrylamide (TLa) 35
9.3.12 Representative Double Modification of TLa-containing copolymer: Aminolysis and Thiol-ene "click" 36
9.3.13 Representative Double Modification of TLa Homopolymer: Aminolysis and Thiol-ene "click" 37
9.3.14 Fluorescence-linked sorbent assay for polymer inhibitory activity 39
9.3.15 Synthesis of pentafluorophenyl 2-(dodecylthiocarbonothioylthio)-2-methylpropionic acid (PFP-DMP/PFP-DDMAT) 40
9.3.16 General Procedure for Synthesis of PFP-pHEA polymer 40
9.3.17 General Procedure for Synthesis of BG-pHEA polymer 41
9.3.18 General Procedure for Synthesis Polymer-Coated Gold Nanoparticles (PFP-pHEA- or BG-pHEA-AuNPs) 42
9.3.19 Synthesis of 1-b-propargyl-D-galactose 43
9.3.20 (Unsuccessful) Azide-modification of Poly(3-hexylthiophene-2,5-diyl)-Br (P3HT-Br) with Sodium Azide 43
9.3.21 Azide-modification of Poly(3-hexylthiophene-2,5-diyl)-Br (P3HT-Br) 44

10 Bibliography 45

3 Introduction

Of particular interest to the biomaterials chemist are new realms in which polymeric materials can be modified to interact with biomolecules.[1,2] *In vivo* visualisation of these interactions is also vital to understanding the chemical basis for them, and in designing of further small molecules or polymers with greater affinity for detrimentally-active molecules.[3–6]

3.1 Glycans and Anti-Adhesion Therapy

Glycans are saccharide chains often found on the surface of human or bacterial cells, or as protein modification.[7] Thus, they are used in many essential cell-surface interactions such as cell-signalling, fertilisation, and even in the recognition and binding of toxins and bacteria (termed adhesion, see Figure 1).[7–12] Proteins that mediate these processes by binding to the aforementioned glycans are termed lectins; often, especially in the case of plant "agglutinins" these interactions result in cell aggregation (for example, in the binding of bacterial cells).[7,13–15]

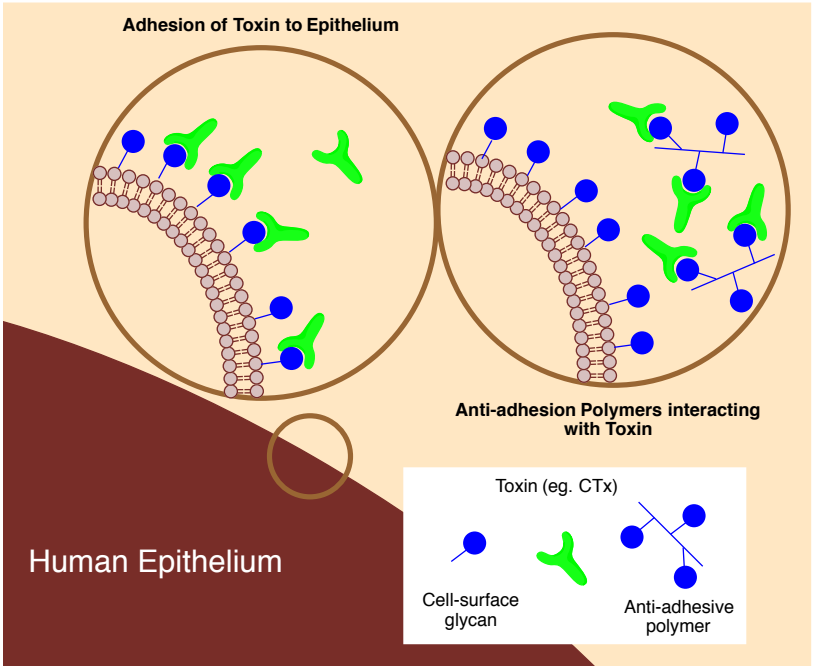

Figure 1: Adhesion and Anti-adhesion interactions of toxin such as CTx.

As the interactions are non-covalent, the triggering of downstream signalling cascades require the "cluster glycoside" effect, wherein the binding constant is amplified as a sum of the total ligand number, and thus is greater than the sum of individual glycan affinities.[11,16–18] The use of polymers with saccharides attached at multiple sites along the polymeric chain can exploit this effect to enhance binding affinity. The use of such glycopolymers to out-compete the binding of toxins to the human cell is termed anti-adhesion therapy.[5,6,15,19]

Small molecule inhibitiors have been developed previously for anti-adhesion therapy, with high affinity in their binding due to a good fit in the toxin's sugar binding pocket, utilising structural biology studies.[15] Further work, however, has often used polymeric materials to benefit from the aforementioned cluster glycoside effect.[5,6,16,19]

Glycoconjugate anti-infectives have been developed to target a colossal array of lectins such as DC-SIGN or galectins in HIV therapy and bacterial Shiga toxins.[20–22] An important target for multivalent anti-adhesion therapy is the toxin CTx, secreted by *Vibrio cholera*, the cause of 28,000 – 142,000 deaths every year.[23–25] CTx is a multimeric AB_5 protein complex, consisting predominantly of 5 B subunits that each bind the GM1-gangliosides (lectins) present on the human epithelial cell surface (see Figure 2).[17,24–27] This binding the first step in a cascade of signalling events resulting in infection with *Vibrio cholera*.

Richards et al. have developed various anti-adhesive galactose glycopolymers.[5,6] These were synthesized by tandem post-polymerisation modification in order to finely tune the carbohydrate density as well as the polymer chain and linker lengths. From the library of glycopolymers synthesized, those with the most affinity for CTx turned out to be those with longer linker lengths in order to sit neatly in CTx's deep galactose-binding pocket.[5,26] In addition to this, those with a lower density of galactose residues (10% rather than 50%) had a higher affinity. Galactose-functional inhibitors have been developed with high CTx affinity, but specificity still poses a challenge to avoid interaction with other lectins, such as the mammalian galectins, which could cause unwanted immune response.[6]

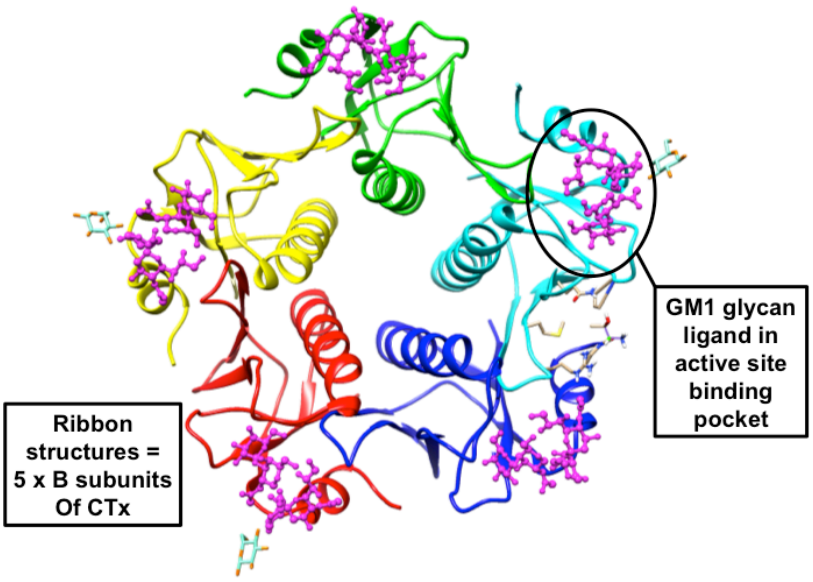

Figure 2: GM1 ligand binding to CTx protein.

3.2 Reversible Addition- Fragmentation Atom Transfer Polymerisation for Controlled Glycopolymer Structure

There are various strategies in the polymer chemist's toolbox for synthesizing glycopolymers with controlled structure. For both safety reasons and to enhance understanding the chemical basis of biomolecule interactions, we ideally want to introduce only polymeric materials of known length, structures and functionality into living systems.[28–31]

Reversible Addition-Fragmentation chain Transfer (RAFT) polymerisation is often used for these purposes.[29–34] This controlled polymerisation method acts to reversibly deactivate the propagating radical chain end to effectively lower the radical concentration and reduce termination and transfer reactions to zero (see Figure 3). This is typically achieved with sulphur containing compounds including dithioesters, trithiocarbonates and xanthates, termed chain transfer agents (CTAs).[28,30,35,36] RAFT is an extremely versatile controlled polymerisation technique as it tolerates a vast array of reaction conditions, monomers and functionalities, whilst producing polymers of narrow molecular weight distribution.[30] The chain transfer agent in this work was selected to be incredibly tolerant of acrylamides, and yielding of good control.[35]

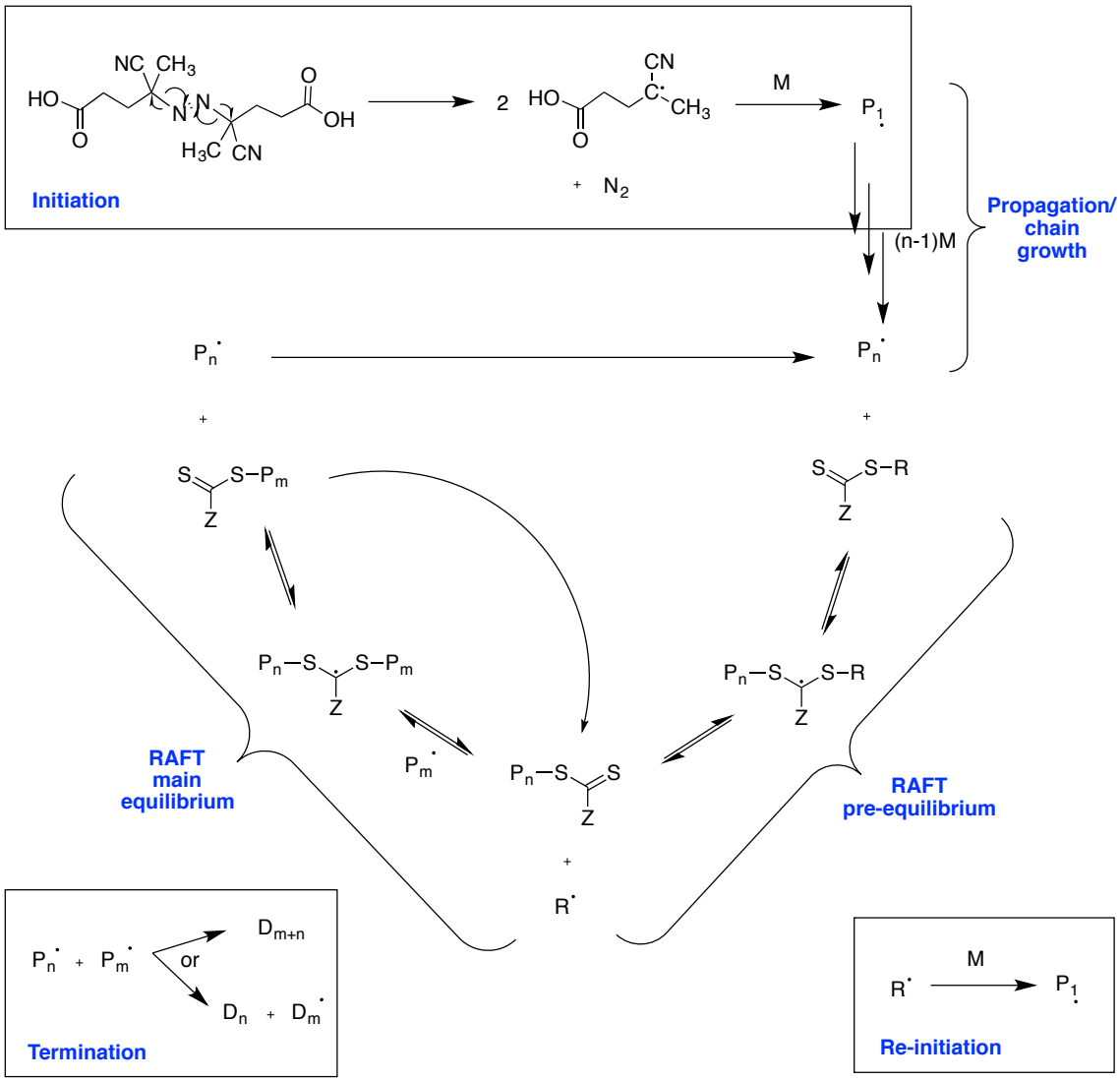

Figure 3: Scheme of RAFT Polymerisation technique.

The use of glycomonomers in polymer synthesis requires protecting group chemistry to avoid undesired side reactions involving the sugar moieties. These chemistries therefore introduce additional deprotection steps that can lead to lower yields.[11,37] Consequently, it follows that post-polymerisation strategies are often preferred.[38,37,39–43] Post-polymerization strategies enable the synthesis of a single modifiable polymer scaffold, with one molecular weight distribution, to which a range of functionalities can be applied. As avidity (binding strength) changes with polymer size, this is essential to avoid confounding the different factors contributing to biological activity. These modifications are particularly attractive where 100% functionality is not required (or, in the case of this work, even desired). There are several versatile methods frequently implemented in the post-polymerization glycosylation of polymers (see Figure 4).[38,37,39–44]

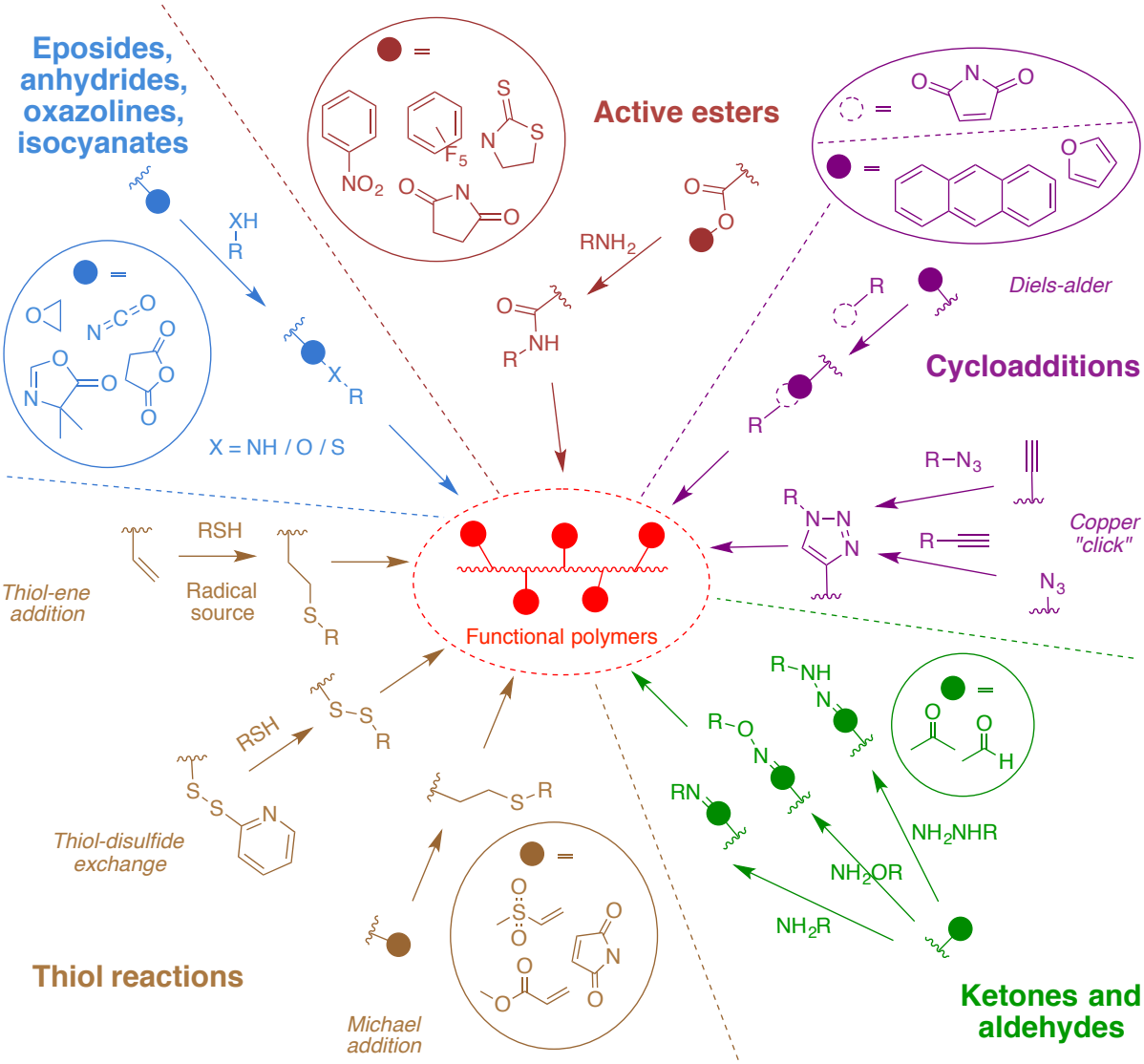

Figure 4: Common strategies used in post-polymerisation, partially adapted from reference 39.

All these methods are viable for introduction of galactose or other sugar moieties, and have, crucially, been successfully implemented in previous anti-adhesion work with Cholera.[5,6] In this work, however, the introduction of a second modification was attempted to potentially enhance affinity through the exploitation of both the *N*-acetyl neuraminic acid and galactose binding sites present on CTx. "Click" chemistry is desirable for its versatility (allowing the application of many functionalities to one polymer scaffold), facility and high yields.

3.3 Modifiable *N*-Thiolactone Acrylamide Polymers

A polymeric mimickry of the structure of GM1 (CTx's chosen ligand) requires a linker with galactose at the end, and *N*-acetyl neuraminic acid at a shorter branch.[26] The usage of a doubly modified side chain rather than a random heteropolymer allows control over the spacing of the added functionalities to enhance affinity (see Figure 5).

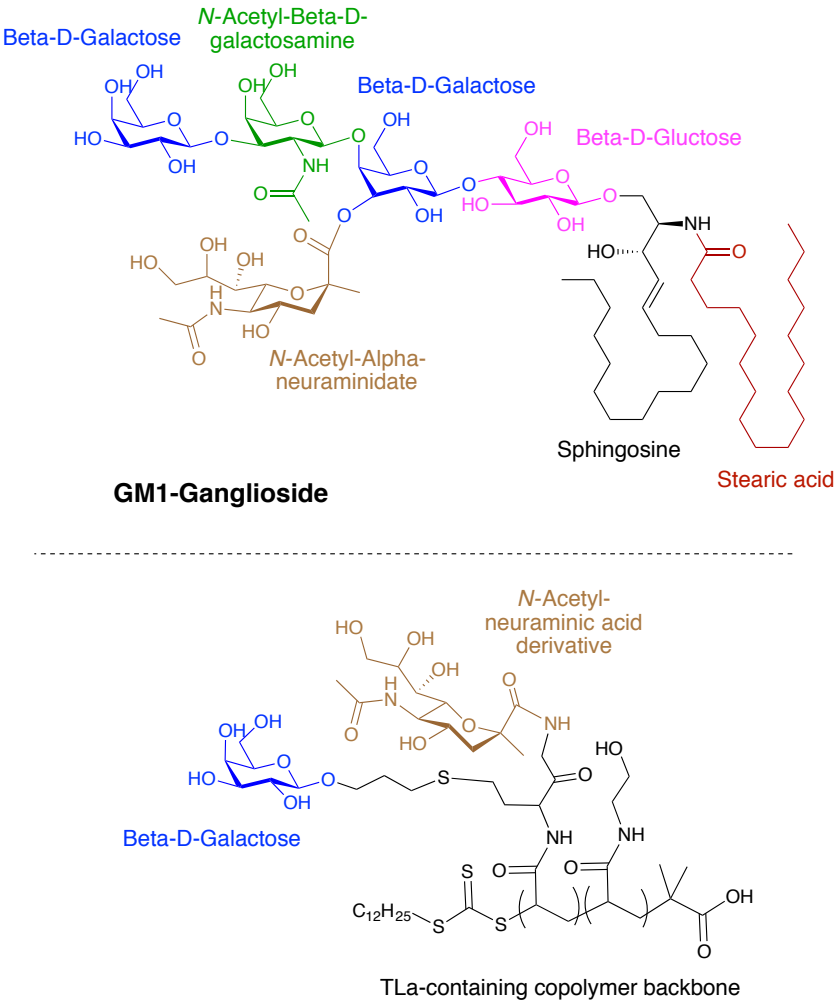

Figure 5: Structure of GM1-ganglioside, and "ideal" doubly-modified polymer.

A method widely implemented by the Du Prez group is the use of *N*-thiolactone monomers: of interest to this study would be the *N*-thiolactone acrylamide (TLa) monomer.[45–52,36,53] These monomers have been used in various RAFT copolymerisations: with *N*-isopropyl acrylamide to enable fine-tuning of its cloud point, for example.[45,53] Subsequently to their copolymerisation, the thiolactone ring can be opened by treatment with a primary amine, which liberates a thiol moiety. The aminolysis step can introduce one new moiety, whilst Michael addition at the subsequently-released thiol can introduce a second.[45,53]

Due to the depth of the CTx binding pocket, galactose functionality should be added to the thiol (at the end of the longer side chain), with various functionalities explored for addition at the aminolysis stage.[26] This work will attempt copolymerisation with *N*-hydroxyethyl acrylamide (HEA) as poly-*N*-hydroxyethyl acrylamide (pHEA) is a polymer shown previously to be well-tolerated in the human body; essential in work leading to internal use.[34,54]

In order to functionalise the TLa units of the polymer, amino- and allyl moieties are required (see Figure 6). The former, amino-sugars, are facile to synthesize with ammonium salts and just the relevant reducing sugar in solution in air.[55,56] The latter can be achieved simply through the use of boron trifluoride as a catalyst for nucleophilic attack of an alcohol on the acetyl-protected galactose sugar's anomeric position using an alcohol, again in air.[34,57]

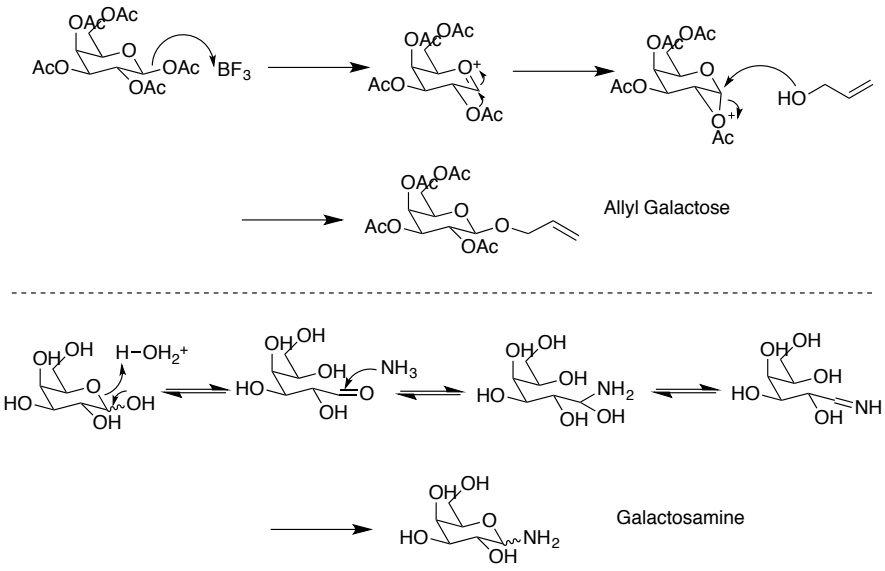

Figure 6: Synthesis of allyl and amino-sugars.

CTx inhibition of the modified polymers may be assessed through a fluorescence-linked assay previously used to determine binding of the polymers to CTx relative to GM1.[5]

3.4 Gold Nanoparticles as a Scaffold for Protein-Polymer Conjugates

Gold nanoparticles (AuNPs) have been widely used in the visualisation of polymer-protein interactions.[3,4,58] The coating of colloidal AuNPs with glycopolymers both enhances stability of the particles in buffer and can confer functionality; polymers synthesized by RAFT with a thiol-containing CTA have a thiol end group that readily links to the gold surface.[34,58]

Of interest in this work is the potential linkage of a protein tag (SNAP-tag, specifically) through benzylguanine (BG) functionality on AuNPs.[59] Previous work by Richards et al. utilised poly(pentafluorophenyl methacrylate) polymers (the pentafluorophenol, PFP, group conferred by a PFP-CTA) as a scaffold due to the facile conversion of the PFP group into a desired water soluble amine.[5] SNAP-tag is an extensively tag that can be fused to a protein or other molecule via a BG functionality.[59–65] BG-functional AuNPs (prepared through addition of an amino BG) would then link to the desired protein via the SNAP-tag.[59,61]

Photorhabdus is an insect-pathogenic gram-negative bacterium that lives in a symbiotic relationship with the *Heterorhabditis* nematode worm.[66,67] The genome of *Photorhabdus* contains several phage-

related loci, with proteins similar to phage tail and base plate proteins, and putative effector (toxin) proteins.[66–69] The phage-like activity of these "*Photorhabdus* virulence cassettes" (PVCs) has been verified through insecticidal activity in the Wax Moth, using mutagenesis to prove that this was due to the PVCs.[69]

Current work underway in the Waterfield group involves replicating the components of the PVCs separately so that the loading of them and their binding can be specifically modified. Figure 8 shows the visible structure of the PVCs. In particular, the tail-fibres have been implicated in their specific cell binding.[66,69,70] Upon their conjugation to a SNAP-tag, these products could be conjugated to a polymer delivery system to enhance specific binding (see Figure 8).

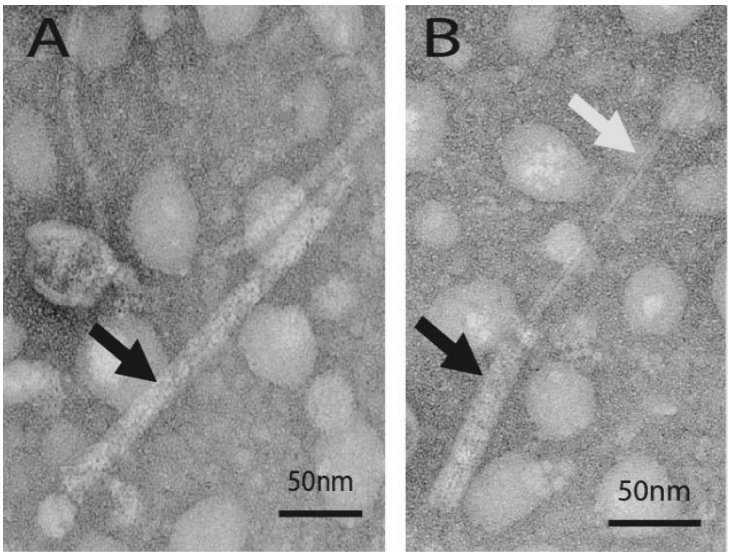

Figure 7: Transmission electron micrographs of PVC products from Reference 64.

(A) Relaxed PVC, showing only the outer "syringe-like" sheath (arrow). (B) Contracted PVC product, showing extrusion of the syringe needle (white arrow) from syringe sheath (black arrow).

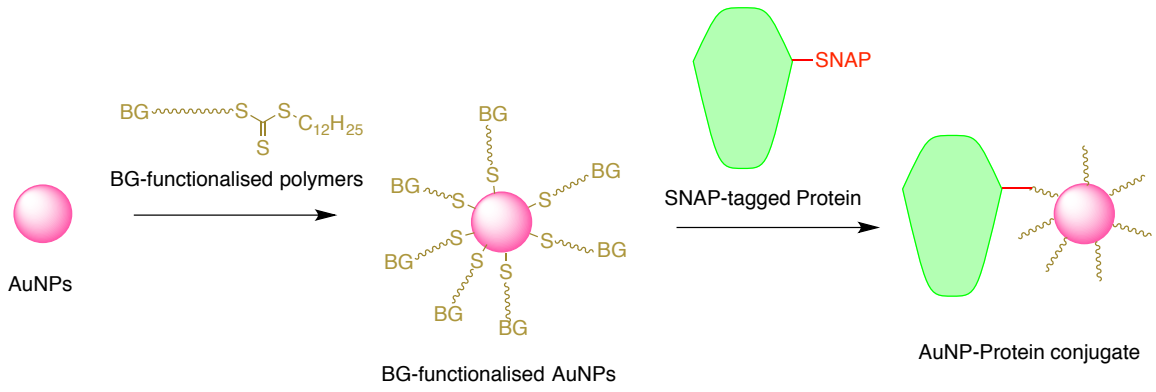

Figure 8: Conjugation of modified polymers to proteins via AuNPs and SNAP-tag.

AuNPs have characteristic optical properties that mean they can be detected label-free.[3,71] UV-Vis measurements can detect their size, shape and degree of aggregation; the latter leading to an intense colour change that can be seen by eye.[3] Test AuNPs functionalised by BG and then SNAP-tag could therefore be detected by a simple UV-Vis experiment with immobilised SNAP-tag-antibody on a microplate.[3]

4 Aims

- To investigate novel RAFT glycopolymer-based materials for use in cholera toxin anti-adhesion.
- To develop alternative strategies for detection of polymer-protein interaction using a UV-visible-active poly(3-hexylthiophene-2,5-diyl) scaffold.
- To use SNAP-tag protein and gold nanoparticles as a potential basis on which to form protein-polymer conjugates.

5 Objectives

- To use RAFT polymerisation techniques to produce polymers and copolymers for use in various protein-polymer interactions.
- To use post-polymerisation modification techniques to add protein-interacting functionalities to the synthesized polymers and copolymers.
- To assess the binding affinity of pHEAA/pTLa polymers and copolymers to the GM-1 adhesion cholera strain.
- To develop a detectable protein binding system using sugar-modified P3HT polymer.

6 Milestones for year 1

- **Literature survey** over previous work in the areas of cholera toxin inhibition, PVC syringes and thiolactone acrylamide.
- **Investigate the use of doubly-modified polymers in the inhibition of cholera toxin**, including the synthesis of modifiable polymers with different quantities of thiolactone monomer units and their post-polymerisation modification with neuraminic acid and galactose using aminolysis and thiol-ene "click" chemistries respectively.
- **Assessment of polymer binding to the CTx cholera toxin strain**, both for the doubly modified polymers and some control polymers I will synthesize using the same chemistries.
- **Synthesis of dyed RAFT polymers** for use in the PVC syringe project. These will then be attached to the head of the syringe using a SNAP-tag; though this work is unlikely to occur this year.
- **Presentation of work at a conference.**

7 Results and Discussion

The GM1-ganglioside binds to cholera toxin (CTx) with high affinity and specificity due to the presence of both a chain-end galactose, and a side-branch sialic acid residue. The sialic acid has little affinity itself for CTx but binds an allosteric site enhancing affinity. An aim of this work is to produce doubly modified polymers as multivalent GM1 mimics, with two sugars in the correct spacial pattern. The thiolactone group can be used to introduce two differing functionalities through the aminolysis of the ring and a thiol-ene ('click') step (see Figure 9). These functionalities can further mimic GM1 through their spacing – with the thiol-ene modification at the chain end (as with GM1's galactose) and the aminolysis as a side-branch (as with GM1's sialic acid).

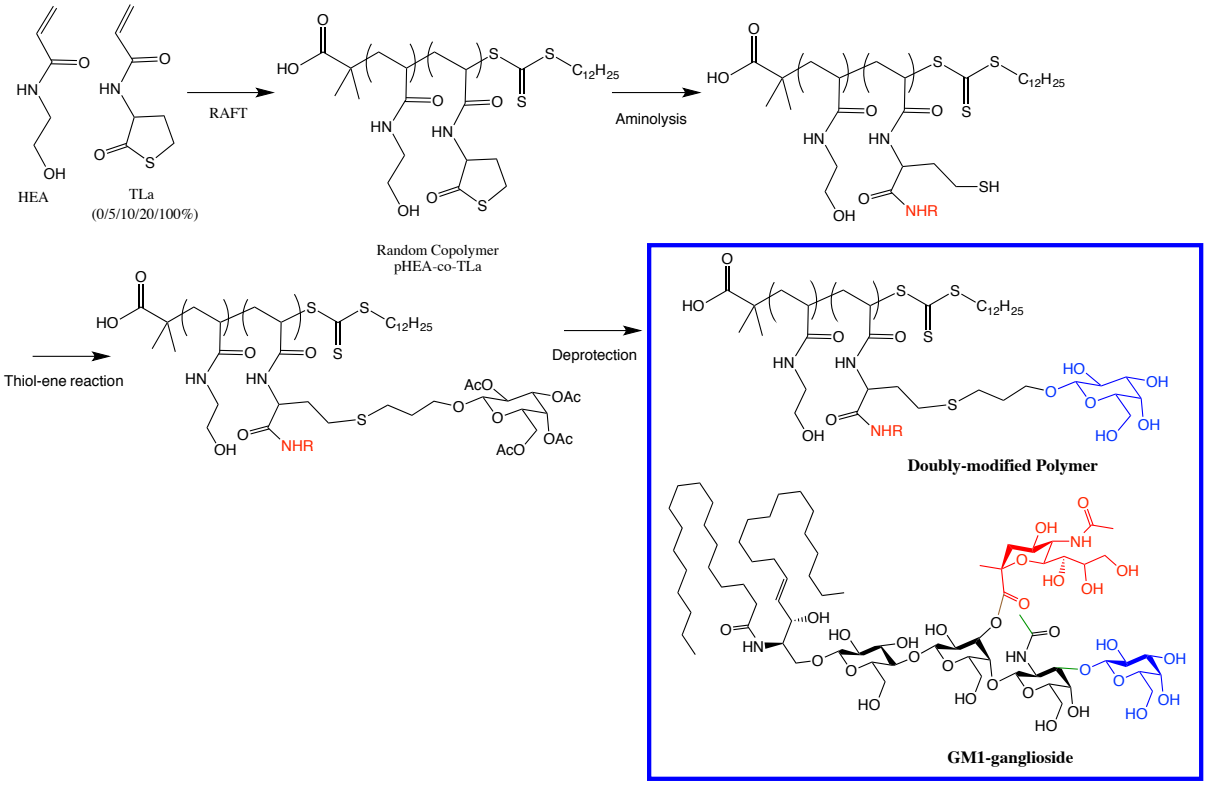

Figure 9: Scheme for synthesis of doubly modified GM1 mimic.

7.1 Synthesis of Doubly-Modified Polymers

N-hydroxyethyl acrylamide (HEA) / *N*-thiolactone acrylamide (TLa) copolymers were synthesized using a 2-(dodecylthiocarbonothioylthio)-2-methylpropionic acid RAFT agent, with a variety of TLa contents to enable comparison of different functionalization in the final protein-binding assays. Polymers were characterised by DMF-SEC and ^{1}H-NMR. These data are shown in Table 1; conversion was determined as the depletion of the vinyl peak relative to an NMR reference standard (mesitylene), seen as a distinctive singlet in the ^{1}H-NMR spectrum (see Equation E1 and Figure S1). Thiolactone contents of the polymer were verified by depletion of the thiolactone vinyl peaks by ^{1}H-NMR also. As would be expected for a RAFT polymerization, the dispersity values were relatively

low, and the molecular weights obtained by SEC were comparable to those from conversion. Reactivity ratios for TLa and HEA are not known, so there may be some composition drift in the polymer; but as both are methacrylamides, the R values should be relatively similar.

Table 1: Characterisation data of PFP- and BG-pHEAs.

Polymer	% TLa	Conversion (^{1}H-NMR)	[M]:[CTA]	DP[a]	$M_{n(theo)}$[a]	$M_{n(SEC)}$	M_w/M_n (SEC)
pNIPAM	0	72.5	100	72.5	8,209	10920	1.16
pHEA	0	82.6	75	62.3	7,051	13904	1.08
pHEA-co-Tla	5	95.2 (HEA) 99.5 (TLa)	47.5 (HEA) 2.5 (TLa)	35.7 (HEA) 1.9 (TLa)	4,402	8585	1.16
pHEA-co-Tla	10	93.2 (HEA) 98.2 (TLa)	45 (HEA) 5 (TLa)	34.2 (HEA) 3.9 (TLa)	4,540	8912	1.13
pHEA-co-Tla	20	76.3 (HEA) 84.0 (TLa)	80 (HEA) 20 (TLa)	61.1(HEA) 16.8 (TLa)	9,650	9201	1.26
pTLa	100	50	59.9	35.4	3,315	5240	1.11

a: Determined by experimental conversion x ([M]:[CTA])

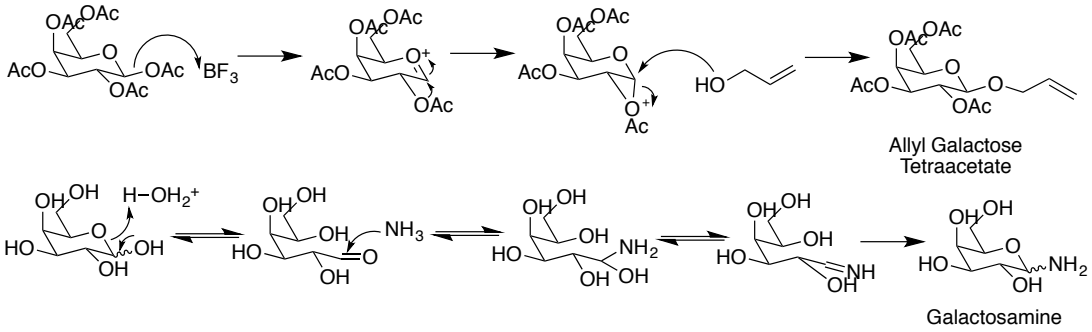

Figure 10: Scheme for synthesis allyl and amino galactose sugars.

Amino and allyl galactose were required for the aminolysis and thiol-ene modifications of the TLa polymers respectively (see Figure 10). The amination of galactose by ammonium carbonate is a convenient method to aminate reducing sugars with no protecting group chemistry required. To obtain allyl galactose, boron trifluoride was used to activate the anomeric acetate on galactose pentaacetate, with allyl alcohol as the nucleophile with neighbouring group participation to promote beta configuration. The synthesis of the amino and allyl galactose was successful, and confirmed by ^{1}H-NMR (see Figures S3 and S4) .

With the library of TLa-containing polymers to hand, and the reactive sugars, the post-polymerisation was conducted. A representative sample of 100 % TLa was used to verify successful modification of

the TLa-containing homo- and copolymers – this representative sample was modified with glucosamine and allyl galactose tetraacetate. A molecular weight increase was observed whilst a low polydispersity was maintained, showing that undesirable side reactions such as disulfide formation (which would increase Mw) did not occur (determined by DMF-SEC using PMMA standards, see Figure S5, Table 2). The presence of glucose/galactose sugar peaks by ^{1}H-NMR also suggested successful modification (see Figure S6) but was not quantified in this case, as this was a test reaction.

Table 2: SEC Data for modified pTLa.

Polymer	$M_{n(SEC)}$	$M_{w(SEC)}$	M_w/M_n
pTLa	5776	6466	1.12
pTLa (modified with glucosamine and allyl galactose tetraacetate)	6260	7043	1.13

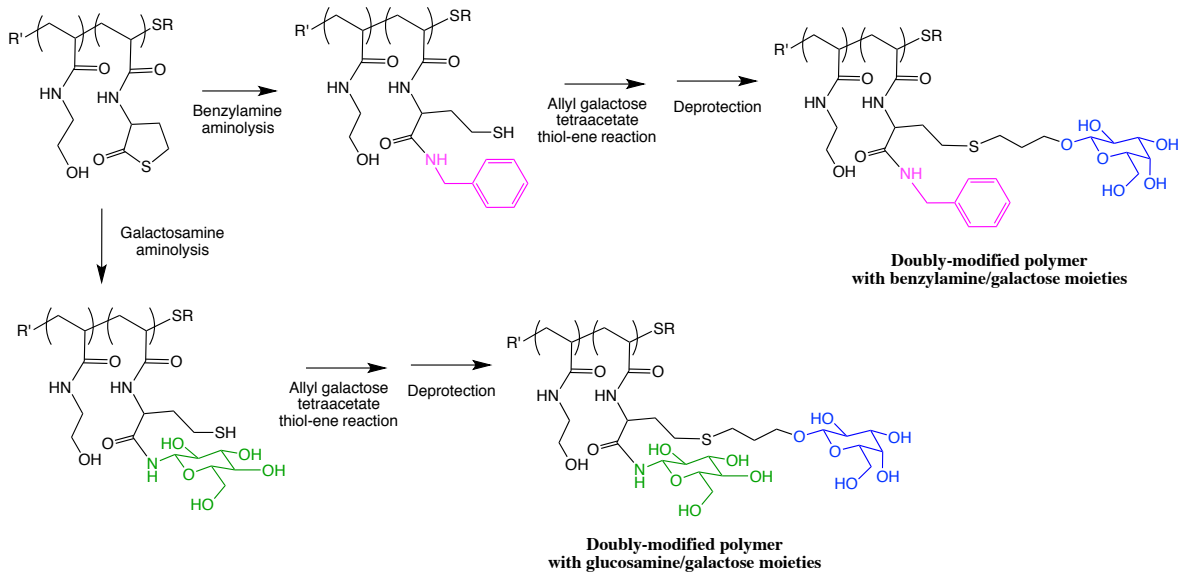

Figure 11: Scheme for synthesis of benzylamine/glucosamine and allyl galactose-modified polymers.

In this investigation, the 5, 10, 20 and 100% TLa polymers were all modified with glucosamine/benzylamine through aminolysis, followed by thiol-ene addition of allyl galactose tetraacetate, and deprotection (see Figure 11). All modified TLa polymers except for the homopolymer were soluble in water, which is essential for all the biological assays. The change in solubility, wherein the modified polymers were soluble in water after the deprotection step but not before, also suggested a successful modification. Infrared spectroscopy confirmed all the TLas as ring opened.

7.2 Inhibitory activity of Doubly-modified Polymers

In order to test for interaction between the modified polymers and CTx protein, docking studies were undertaken using the SwissDock online server. The server gave potential binding sites for the proposed ligands (a single repeat unit of the modified polymer were used for this), with their predicted binding energy (negative energies being more energetically favourable). The proposed dockings were narrowed down to those where the substrate was within the binding site, facing such that the polymer chain would be outside of the active site. The most energetically favourable dockings for the galactosamine/benzylamine-allyl galactose functionalized repeat units are shown in Figure 12. These predictions are not conclusive, and are not necessarily the best predictors of high affinity, as they do not take into account solubility, multivalency or the packing of the polymer chain.

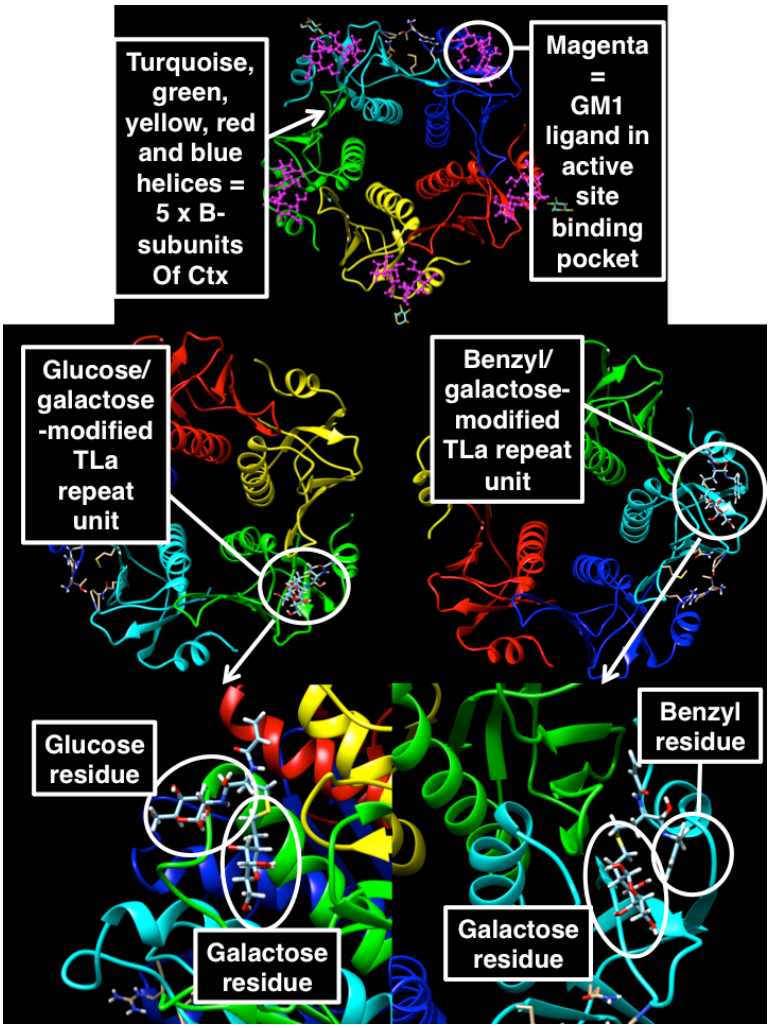

Figure 12: Swiss-Dock binding outputs for glucosamine/allyl galactose and benzylamine/allyl galactose.

These outputs had predicted energy of -1.25 and -3.41 kJ mol^{-1} respectively. In each case, the ligand's galactose residue can be seen clearly in the binding pocket occupied by the GM1 ligand. The second

residue (glucose/benzyl) sits slightly outside of this pocket. The repeat unit backbone sits outside of the active site. Images were generated using UCSF Chimera.

Supported by the docking results, the library of polymers was then used to probe the impact of the double-functional polymers on their ability to inhibit CTx function. Fluorescence-linked sorbent assays were undertaken (see Figures 13-15). In these assays, polymer and CTx-FITC solutions were incubated to allow polymer to bind to the toxin's active site. This solution was then applied to microplates with GM1 on their surface. If the polymers have increased affinity towards CTx, this prevents the CTx binding to its native GM-1 ligand. Therefore, post-washing, a decrease in fluorescence relative to controls with no polymer present indicated more activity.

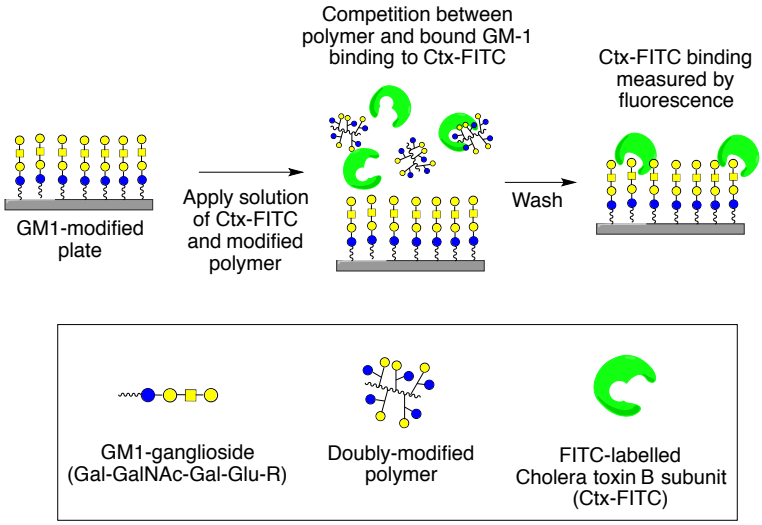

Figure 13: Fluorescence-linked sorbent assays to assess inhibitory activity of modified polymers.

Effective binding curves showing inhibitory activity have sigmoidal shapes, with a lower fluorescence plateau (at higher polymer concentration) where the polymer has inhibitory activity, and a higher fluorescence plateau where inhibition is no longer occurring (at the lower polymer concentrations). The binding curves for polymers that do not have this shape signify that they do not have concentration-dependent inhibitory activity. In these binding assays, 5, 10 and 20% TLa glucosamine-modified polymers were found to have extremely potent inhibitory activity, whilst the benzylamine-modified polymers did not. The benzyl polymers also may have aggregates at higher concentrations, causing precipitation onto the plate and the higher fluorescence signals. The 5 and 10% loadings were more active than the 20% loading, whilst 100% TLa loading did not show inhibitory activity. This activity with the 100% TLa polymers may have been due to its low water solubility, requiring significant amounts of DMSO in the buffer . To fully understand this interaction further, processing is required to take into account the total sugar concentration – low-density polymers at equal mass concentration have fewer sugars, so this must be corrected. Affinities will be calculated in the near future using bilayer interferometry, which is being installed soon.

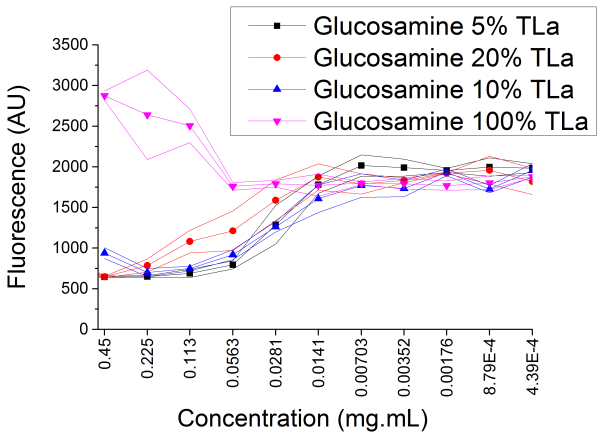

Figure 14: Fluorescence-linked CTx-FITC binding curves for the polymers modified with glucosamine.

IC_{50} values for glucosamine/allyl galactose-modified polymers: 5% TLa = 0.020 mg/mL; 10% TLa = 0.028 mg/mL; 20% TLa = 0.040 mg/mL.

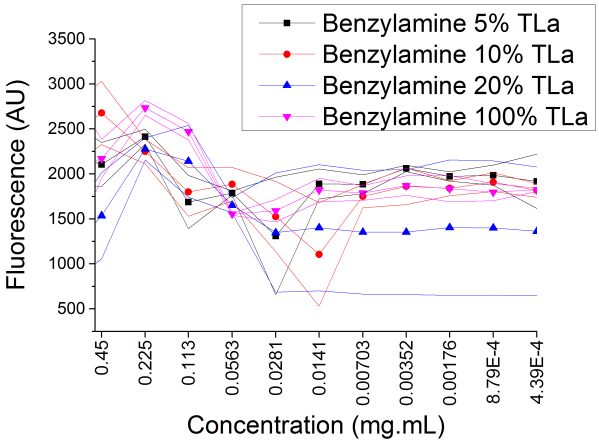

Figure 15: Fluorescence-linked CTx-FITC binding curves for the polymers modified with benzylamine.

7.3 Synthesis of SNAP-tag-able Gold Nanoparticles

An additional part of the PhD is the generation of complex hybrid materials combining synthetic and expressed protein components, described here. Benzylguanine (BG) is a versatile conjugation group with a SNAP-tagged protein. The aim of this investigation is to produce BG-functionalised gold nanoparticles (AuNPs) in order to conjugate them to SNAP-tagged proteins (see Figure 16). This requires the synthesis of BG-functionalised polymers by RAFT, which can in turn be conjugated to AuNPs through the thiol RAFT end group.

In this work, pentafluorophenyl 2-(dodecylthiocarbonothioylthio)-2-methylpropionic acid was used as a chain transfer agent for RAFT polymerisation of HEA. This end group was replaced by an amino

benzylguanine functionality through a facile displacement reaction. The polymer was then conjugated to AuNPs through the thiol end group, requiring only incubation with AuNP citrate solution.

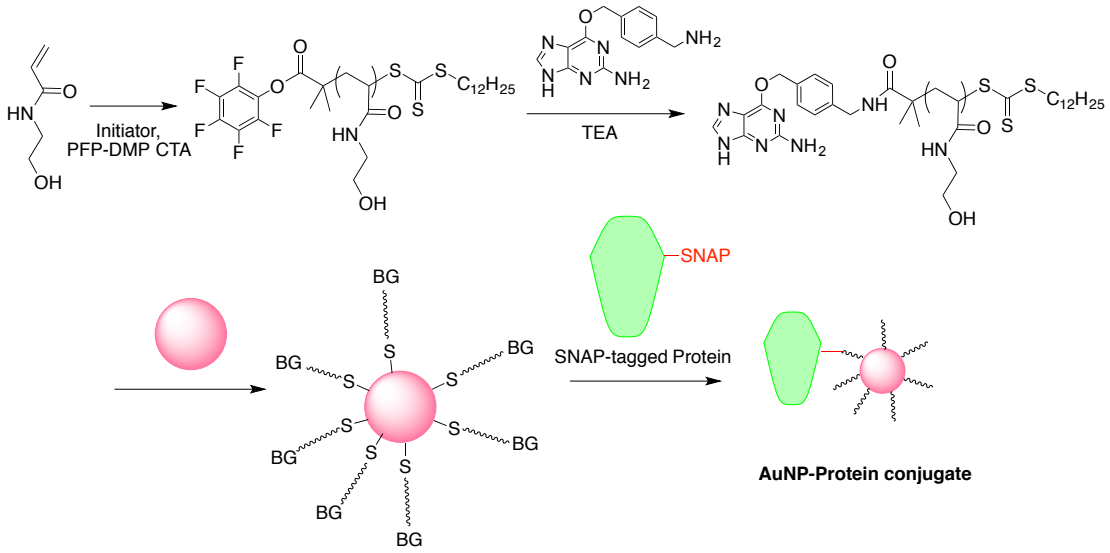

Figure 16: Scheme for synthesis of AuNP-protein conjugate.

N-hydroxyethyl acrylamide with a pentafluorophenol (PFP) end group was successfully polymerised at a variety of degrees of polymerisation and conversion in order to produce a variety of chain lengths. As some of the Mn/Mw data are too high, these experiments need to be repeated (see Table 3).

Table 3: Characterisation data of PFP- and BG-pHEAs.

Polymer	Conversion (^{1}H-NMR)	[M]:[CTA]	DP[a]	$M_{n(theo)}$[a]	$M_{n(SEC)}$	M_w/M_n (SEC)
PFP-pHEA	95.23	100	95.23	11,493	15057	1.33
	95.62	50	47.81	6,035	10563	1.15
	42.83	25	10.71	1,763	4072	1.08
BG-pHEA	-	100	95.23	11,493	19421	1.22
	-	50	47.81	6,035	12960	1.23
	-	25	10.71	1,763	5087	1.25

a: Determined by experimental conversion x ([M]:[CTA])

The existence of the PFP end group was verified by ^{19}F-NMR and FTIR (see Figure S7). These characterisations also show the loss of the PFP group after benzylguanine (BG) functionalization (see Figure S7).

AuNPs were coated with the PFP- and BG-functionalised pHEA by a simple mixing procedure. Their size and stability was investigated by dynamic light scattering (DLS), shown in Figure 17. The

increase in size by DLS signifies a successful coating of the AuNPs with polymer. The distributions with second, higher radius, peaks (or only higher radius peaks) than would be expected for the 15 or 40 nm AuNPs have aggregated due to instability (see DP25 BG-pHEA coated 15 nm AuNPs in particular). Aggregation can also be seen by eye as a change in colour from red to blue (see Figure S8).

This data suggested that the longer chain lengths of polymer, and larger nanoparticle sizes, were the most stable; potentially due a more thoroughly covered AuNP surface. The BG-functionalised nanoparticles were shown to be larger and less stable than those with the smaller, PFP, end group. This could be due to the difference in packing of the polymers close to the AuNP surface with the different end groups and the relative hydrophobicity of the BG groups.

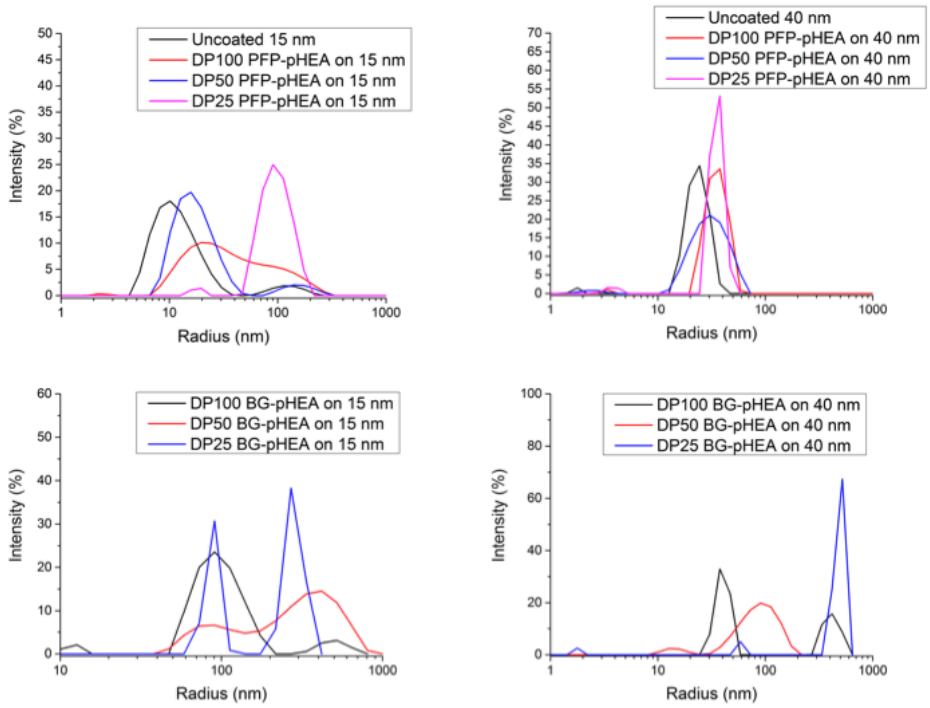

Figure 17: DLS characterisation of polymer-conjugated AuNPs.

7.4 Conclusions

In summary, doubly modified, low dispersity pTLa polymers were synthesized through facile post-polymerisation modification of the thiolactone ring. Fluorescence-linked binding assays showed that 5, 10 and 20% TLa-loaded polymers modified with glucosamine and allyl galactose had inhibitory activity with the CTx protein. These polymers could thus prove to be potential lead structures for new anti-infective treatments

In addition to this work, BG-functionalised polymers were functionalised by the displacement of a RAFT CTA's PFP end group with amino-benzylguanine. These were conjugated to AuNPs, with

longer polymer chain length and greater AuNP sizes proving to be most stable. This work aims to produce BG-functionalised AuNPs in order to conjugate them in the future to SNAP-tagged proteins to enable them to instil further functionality to the proteins.

8 Future work

- **Further investigate double modification of TLa-containing polymers for CTx assays**, potentially attempting further functionalisations or using dialysis for purification rather than precipitation. This work may lead to further Fluorescence-linked sorbent assays.
- **Complete RCA control fluorescence plate assays.**
- **Synthesis of SNAP-conjugated AuNPs to determine whether this is feasible for the *Photorhabdus* work.** These should be tested via fluorescence assays with SNAP-antibody. If this succeeds, generate AuNP-protein conjugates via a SNAP-tag. Potentially also test specific binding of these conjugates to cells.
- **Synthesize P3HT-sugar conjugates via alkyne-azide coupling.** The first step will be to assess bromide displacement by azide with a large alkyne that could be detected by MALDI. My sugar-alkyne could then be added and deprotected. These conjugates, should also be tested for any binding activity with proteins. This will depend strongly on solubility in appropriate solvent.
- **Perform binding assays of polymers to proteins on Octet device.**
- **Presentation of work at a conference.**

9 Materials and Methods

9.1 Materials

Ultra-pure water with resistance < 18 Ω, was obtained from a Milli-Q© Integral Water Purification System. All chemicals were purchased from Sigma-Aldrich and used as supplied unless otherwise stated. 15 and 40 nm citrate-stabilised gold colloid solution was purchased from BBI solutions. *N*-acetylneuraminic acid, D-galactosamine HCl, GM1-ganglioside and 6-((4-(aminomethyl)benzyl)oxy)-7H-purin-2-amine were purchased from Carbosynth. Toluene-d_8 was purchased from Fisher Scientific (all other deuterated solvent used (methanol, chloroform, water) were purchased from Sigma-Aldrich). *n*-Hexane, THF, DMF and ethyl acetate were purchased from Fisher. The cholera toxin used in assays was Cholera toxin B subunt, FITC onjugate, lyophilized powder from Sigma-Aldrich. P3HT-Br polymer was synthesized by Paul Topham's Group in Aston University, Birmingham. HEPES buffer stock solution was prepared with the following concentrations, and adjusted to pH 7.5 using the minimum volume required of 0.1 M $HCl_{(aq)}$ and 0.1 M $NaOH_{(aq)}$: 10mM HEPES, 0.15 M NaCl, 0.1 mM $CaCl_2$ and 0.01 mM Mn^{2+}.

9.2 Analytical Methods

^{1}H, ^{13}C and ^{19}F-NMR spectra were obtained using a Bruker DPX-400 or Bruker DPX-300 NMR Spectrometer; all chemical shifts are reported in ppm (δ) relative to residual non-deuterated solvent. Mass spectrometry was carried out in pure methanol or water on the Agilent 6130B ESI-Quad instrument using electrospray in positive mode. MALDI mass spectrometry was conducted on a Bruker Ultraflex Autoflex Speed MALDI TOF instrument, using DCTB (trans-2-[3-(4-tert-Butylphenyl)-2-methyl-2-propenylidene]malononitrile) as the matrix (10 mg/mL in acetonitrile); the layer method was utilised for all MALDI preparations.[75] FTIR spectroscopy was carried out on a Bruker Vector 22 FTIR spectrometer with a Golden gate diamond attenuated total reflection cell. SEC (GPC) measurements were carried out on a Varian 390-LC MDS system equipped with a PL-AS RT/MT2 autosampler, a PL-gel 3 µm (50 x 7.5 mm) guard column, two PL-gel 5 µm (300 x 7.5 mm) mixed-D columns held at 30°C and the instrument equipped with a differential refractive index and a Shimadzu SPD- M20A diode array detector. SEC samples were filtered through PTFE syringe filters 0.22 microM, 13 mm, from Gilson Scientific. Tetrahydrofuran (with 2% Triethylamine) or Dimethylformamide eluent was used at 1mL.min-1 flow rate. Data were analysed using Agilent GPC software and molecular weight determined relative to narrow molecular weight PMMA standards (200 - 1.0 x 106 g.mol-1). Nanoparticle size was determined using Dynamic Light Scattering (DLS), performed on a Malvern Instruments Zetasizer Nano- ZS with 4mW HeNe laser 632.8 nm. UV/Vis spectroscopy and fluorescence plate readings were performed on a BioTek Synergy HT Microplate Reader.

9.3 Synthetic Methods

9.3.1 Synthesis of 2-(dodecylthiocarbonothioylthio)-2-methylpropionic acid (DMP/DDMAT)

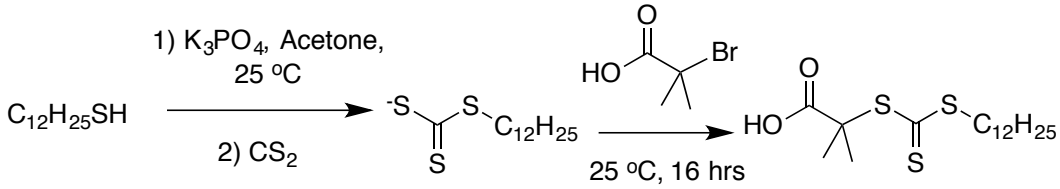

Dodecane thiol (4.75 mL, 19.8 mmol) was added dropwise to a stirred suspension of K_3PO_4 (4.02g, 18.9 mmol) in acetone (60 mL). The reaction vessel was placed in an ice bath. Carbon disulfide (3.20 mL, 53.0 mmol) was added and the solution turned bright yellow, but was still cloudy. After stirring for ten minutes, 2-bromo-2- methylpropionic acid (3.00 g, 18.0 mmol) was added and a precipitation of KBr was noted. The ice bath was removed after 10 minutes and the reaction was left stirring at room temperature for 16 hours. Solvent was removed *in vacuo* and the residue was extracted into DCM (2 x 50 mL) from 1 M HCl (100 mL). The organic extracts were further washed with water (100 mL) and brine (100 mL) and dried over $MgSO_4$. Recrystallisation from n-hexane yielded a bright yellow solid (1.80 g, 27.5%).

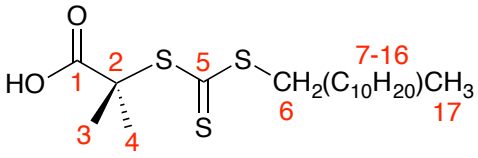

^{1}H NMR (400 MHz, $CDCl_3$) δ_{ppm}: 3.28 (2H, t, J_{HH}=7.5, H6); 1.66 (6H, s, H3/4); 1.10-1.25 (20H, alkyl, H7-16); 0.79 (3H, m, H17).

^{13}C NMR (400 MHz, $CDCl_3$) δ_{ppm}: 220.86 (C5); 178.04 (C1); 55.51 (C2); 37.08 (C7); 31.92 (C6); 29.64, 29.57, 29.46, 29.35, 29.12, 28.98, 27.82 (C8-15); 25.23 (C3/4); 22.70 (C16); 14.13 (C17).

FTIR (solid, ν_{max}/cm^{-1}): 2910 (CH_2); 1710 (C=O); 1440 (C-C); 1305 (C-O); 1070 (S-(C=S)-S).

ESI-MS, positive mode (m/z): 365.2 ($M+H^+$, expected 365.63), 387.1 ($M+Na^+$, expected 387.61).

9.3.2 Synthesis of *N*-Thiolactone Acrylamide

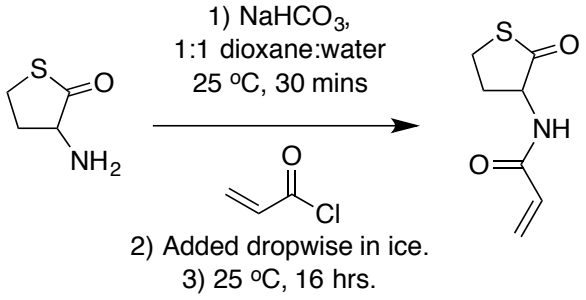

D,L-homocysteine thiolactone hydrochloride (7.04 g, 45.6 mmol) was dissolved in 1:1 dioxane: water (100 mL). The reaction vessel was transferred to an ice bath, and sodium hydrogen carbonate (19.2 g, 228 mmol) was added whilst stirring. After 30 mins stirring, acryloyl chloride (7.45 mL, 91.2 mmol) was added dropwise. The reaction was stirred for 16 hours at room temperature. The reaction was extracted into ethyl acetate (200 mL) from brine (200 mL). The organic layer was dried over Na_2SO_4, filtered and concentrated *in vacuo* to yield a white solid (5.57 g, 71.3%).

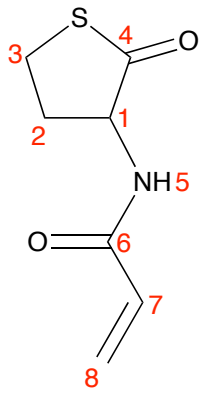

^{1}H NMR (400 MHz, $CDCl_3$) δ_{ppm}: 6.35 (1H, m, H7); 6.17 (1H, m, H8, trans); 5.73 (1H, m, H8, cis); 4.61 (1H, s, H1); 3.41 (1H, m, H3); 3.3 (1H, m, H3); 3.02 (1H, m, H2); 1.99 (1H, qd, J_{HH}=12.5(x3), 6.9, H2).

^{13}C NMR (400 MHz, $CDCl_3$) δ_{ppm}: 165.83 (C), 129.93 (CH, C1), 127.73 (CH_2, C3), 59.59 (CH, C6), 32.07 (CH_2, C7), 27.70 (CH_2, C3).

FTIR (solid, ν_{max}/cm^{-1}): 3290 (N-H); 2900 (CH_2); 1680 (C=O); 1560 (N-H); 1405 (C-C stretch in ring); 1210 (C-N aliphatic); 1005 (=C-H bend); 930 (N-H wag).

ESI-MS, positive mode (m/z): 194.0 ($M+Na^+$, expected 194.20), 365.0 ($2M+Na^+$, expected 365.41)

9.3.3 Synthesis of b-D-galactose pentaacetate

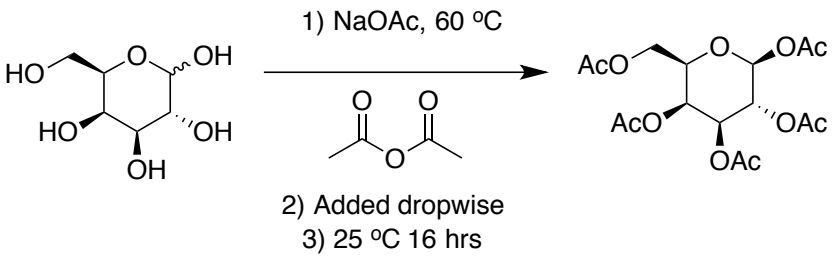

Sodium acetate trihydride (2.06 g, 20.2 mmol) was ground by mortar and pestle and stirred in a 60°C oil bath. D(+)-galactose (2.00 g, 11.1 mmol) was added, and a condenser was attached to the reaction vessel. Acetic anhydride (10 mL, 106 mmol) was added dropwise. The reaction was refluxed for 10 minutes, after which it was cooled to room temperature and left stirring overnight. Ethanol (22 mL)

was added to evolve acetic acid. The mixture was concentrated *in vacuo*, extracted into DCM (40 mL) and washed with warm water (2 x 40 mL). The organic layer was dried over $MgSO_4$, filtered and concentrated in vacuo. Ethanol (25 mL) was added, as was a few spatulas of activated charcoal, and the reaction was refluxed for 20 mins, cooled, filtered and recrystallized in ethanol to yield white crystals (1.30 g, 30%).[76]

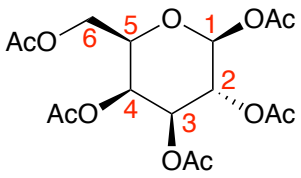

^{1}H NMR (300 MHz, $CDCl_3$) δ_{ppm}: 5.72 (1H, d, J_{HH}=8.2, H1); 5.45 (1H, br s, H4); 5.36 (1H, t, J_{HH}=9.3 x 2, H2); 5.11 (1H, m, H3); 4.17 (2H, m, H6); 4.07 (1H, m, H5); 2.19, 2.15, 2.07, 2.02 (15H, 4 x s, acetyl groups).

^{13}C NMR (300 MHz, $CDCl_3$) δ_{ppm}: 92.17 (CH, C1), 71.12 (CH, C4), 70.88 (CH, C2), 67.82 (CH, C3), 66.79 (CH, C5), 61.03 (CH_2, C6), 20-21 (CH_3, Acetyls).

FTIR (solid, ν_{max}/cm^{-1}): 2973 (CH_2); 1765 (C=O); 1374 (C-H); 1210 (C-O stretch); 957 (=C-H bend); 900 (C-H "oop").

ESI-MS, positive mode (m/z): 413.1 ($M+Na^+$, expected 413.33)

9.3.4 Synthesis of 1-b-allyl-D-galactose

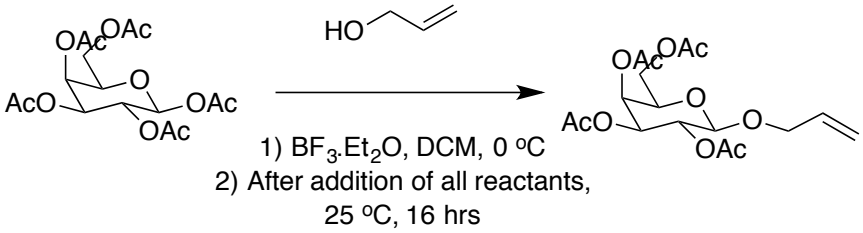

Beta-D-galactose pentaacetate (2.00 g, 5.13 mmol) was dissolved in DCM (40 mL). Allyl alcohol (0.425 mL, 6.25 mmol) was added whilst stirring in an ice bath. Boron trifluoride dietherate (1.35 mL, 7.11 mmol) was added dropwise. 20 minutes later, the reaction was taken out of the ice bath and stirred for 16 hours. Anhydrous potassium carbonate (1.08 g, 7.24 mmol) was added whilst stirring. 30 minutes later, the reaction was filtered and washed with water (2 x 50 mL) and brine (50 mL). The organic layer was dried over $MgSO_4$, filtered and concentrated *in vacuo*. The residue was purified by column chromatography on silica using an eluent comprising 2:3 ethyl acetate: 40 – 60 °C petroleum ether to yield a yellow oil (1.02 g, 51.2%)

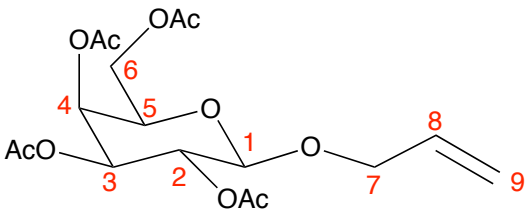

^{1}H NMR (300 MHz, $CDCl_3$) δ_{ppm}: 5.88 (1H, m, H8); 5.41 (1H, d, J_{HH}=3.2, H1); 5.34 (1H, m, H4); 5.28 (1H, m, H2); 5.17 (1H, m, H9); 5.05 (1H, m, H3); 4.5 (2H, m, H6); 4.15 (2H, m, H7); 4.13 (1H, m, H5); 2.15, 2.06, 2.05, 1.99 (15H, 4 x s, acetyl groups)

^{13}C NMR (300 MHz, $CDCl_3$) δ_{ppm}: 117.61 (CH_2, C9), 100.12 (CH, C8), 70.96 (CH, C1), 70.67 (CH, C4), 70.04 (CH_2, C7), 69.01 (CH, C2), 67.07 (CH, C3), 61.30 (CH_2, C6), 30.94 (CH, C5), 20-21 (CH_3, Acetyls).

FTIR (solid, ν_{max}/cm^{-1}): 3027 (O-H); 2920 (CH_2); 1754 (C=O); 1495 (C-H); 1220 (C-O stretch); 705 (C-H).

ESI-MS, positive mode (m/z): 411.1 ($M+Na^+$, expected 411.36)

9.3.5 Synthesis of 1-amino-b-D-galactosamine

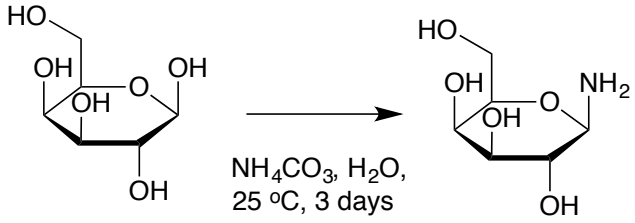

D(+)-Galactose (1.0 g, 5.6 mmol) and ammonium carbonate (5.5 g, 57 mmol) were dissolved in water (25 mL). This was stirred at room temperature for 3 days, with 40 mg per mg of ammonium carbonate added over the course of the reaction to maintain saturation. The reaction was then freeze-dried to remove the ammonia, and subsequently stirred in warm methanol (40 mL) to evolve CO_2. A white powder was obtained through concentration *in vacuo* (0.650 g, 54%).

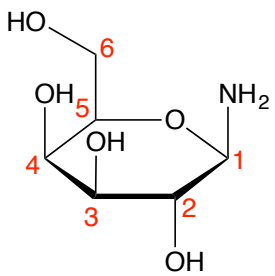

^{1}H NMR (400 MHz, D_2O) δ_{ppm}: 3.94 (1H, d, J_{HH}=8.8, H1); 3.84 (1H, d, J_{HH}=3.3, H4); 3.64 (2H, m, H2/3); 3.56 (2H, m, H6); 3.30 (1H, m, H5).

^{13}C NMR (400 MHz, D_2O) δ_{ppm}: 85.49 (CH, C1), 75.96 (CH, C4), 73.39 (CH, C2), 71.97 (CH, C3), 68.96 (CH_2, C6), 61.16 (CH, C5).

FTIR (solid, ν_{max}/cm^{-1}): 3000 (O-H); 1615 (N-H); 1505 (C-C in ring); 1312 (C-O); 999 (O-H).

ESI-MS (m/z): 381.1 ($2M+Na^+$, expected 381.33).

9.3.6 (Unsuccessful) Synthesis of Amino-Sialic Acid

Sialic acid (N-acetyl neuraminic acid) (1.0 g, 3.2 mmol) and ammonium carbonate (3.1 g, 32 mmol) were dissolved in water (30 mL). This was stirred at room temperature for 3 days, with 40 mg per mg of ammonium carbonate added over the course of the reaction to maintain saturation. The reaction was then freeze-dried to remove the ammonia, and subsequently stirred in warm methanol (40 mL) to evolve CO_2. A white powder was obtained through concentration *in vacuo*. As this reaction was unsuccessful, no successful characterisation data is available. Although some mass spectra suggested the possible presence of the desired product, no conclusive NMR or IR data supported this.

9.3.7 General Procedure for Polymerisation of *N*-hydroxyethyl acrylamide (HEA)

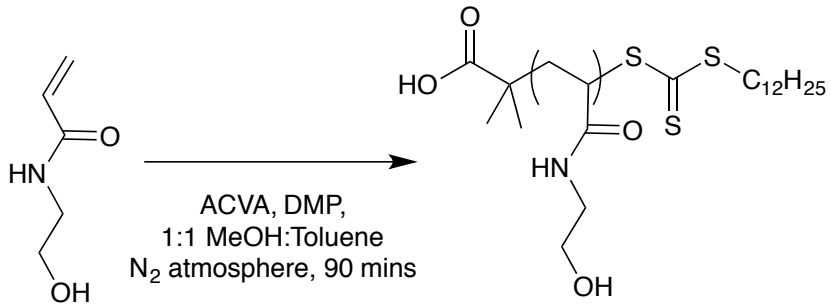

The following procedure describes a reaction with a theoretical degree of polymerisation (DP) of 100 repeat units. 4,4-azobis(4-cyanovaleric acid) (5 mg, 0.018 mmol), 2- (dodecylthiocarbonothioylthio)-2-methylpropanoic acid (CTA, 32 mg, 0.088 mmol) and *N*-hydroxyethyl acrylamide (1 g, 8.8 mmol) were dissolved in 1:1 methanol: toluene (4 mL) in a glass vial with a stirrer bar. Mesitylene (200 µL) was added and a sample was removed for ^{1}H-NMR analysis in $CDCl_3$. The reaction mixture was degassed by N_2 for 30 minutes, sealed and placed in a 70°C oil bath. After 90 minutes, the solution was opened to air and quenched in $N_{2(l)}$. The polymer (pHEA) was precipitated three times from methanol into diethyl ether to give a light yellow solid.

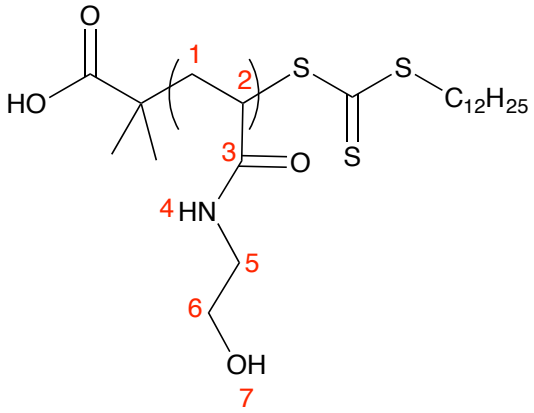

Conversion (NMR): 83.6%; M_n (theoretical): 7051 g.mol^{-1}; M_n (SEC) 13904 g.mol^{-1}; M_w (SEC) 14969 g.mol^{-1}; M_w/M_n (SEC): 1.08.

^{1}H NMR (300 MHz, D_4-MeOH) δ_{ppm}: 4.60-4.90 (br s, H6), 3.55-3.75 and 3.05-3.20 (2 x br s, H5), 2.00-2.20 and 1.50-1.80 (2 x br s, H1/2).

FTIR (solid, ν_{max}/cm^{-1}) = 3300 (N-H and O-H stretch), 2854 (alkyl C-H stretch), 1641 (amide C=O stretch), 1555 (N-H bend), 1443 (alkane), 1225 (C-O stretch), 1060 (C-O stretch).

9.3.8 General Procedure for Polymerisation of *N*-isopropyl acrylamide (NIPAM)

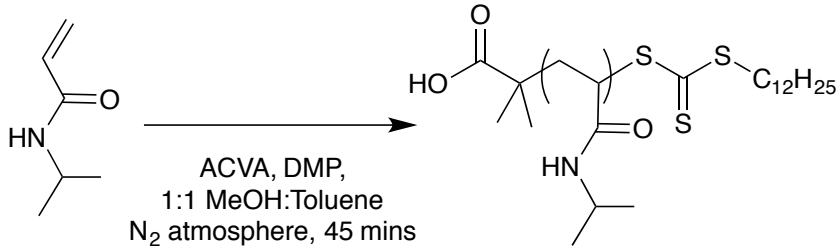

The following procedure describes a reaction with a theoretical degree of polymerisation (DP) of 50 repeat units. 4,4-azobis(4-cyanovaleric acid) (2.5 mg, 0.0089 mmol), 2-(dodecylthiocarbonothioylthio)-2-methylpropanoic acid (CTA, 16 mg, 0.044 mmol) and *N*-isopropyl acrylamide (0.25 g, 2.2 mmol) were dissolved in 1:1 methanol: toluene (2 mL) in a glass vial with a stirrer bar. Mesitylene (100 µL) was added and a sample was removed for ^{1}H-NMR analysis in $CDCl_3$. The reaction mixture was degassed by N_2 for 30 minutes, sealed and placed in a 70°C oil bath. After 45 minutes, the solution was opened to air and quenched in $N_{2(l)}$. The polymer (pNIPAM) was precipitated three times from methanol into diethyl ether to give a light yellow solid.

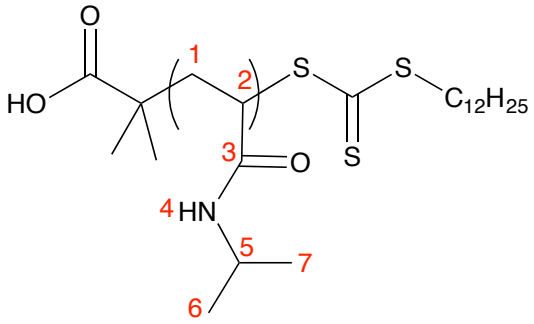

Conversion (NMR): 83.6%; Mn (theoretical): 8209 g.mol-1; Mn (SEC) 10920 g.mol-1; Mw (SEC) 12704 g.mol-1; Mw/Mn (SEC): 1.16.

1H NMR (400 MHz, CDCl3) δppm: 6-6.75 (br s, H4), 3.9-4.15 (br s, H5), 2.0-2.5 (br s, H2), 1.5-1.95 (br m, H1), 1.1-1.4 (br s, H6/7).

FTIR (solid, νmax/cm-1) = 3200 (N-H); 2900 (CH2); 1650 (C=O); 1550 (N-H bend); 1190 (C-H).

9.3.9 General Procedure for Copolymerisation of *N*-hydroxyethyl acrylamide (HEA) and *N*-thiolactone acrylamide (TLa)

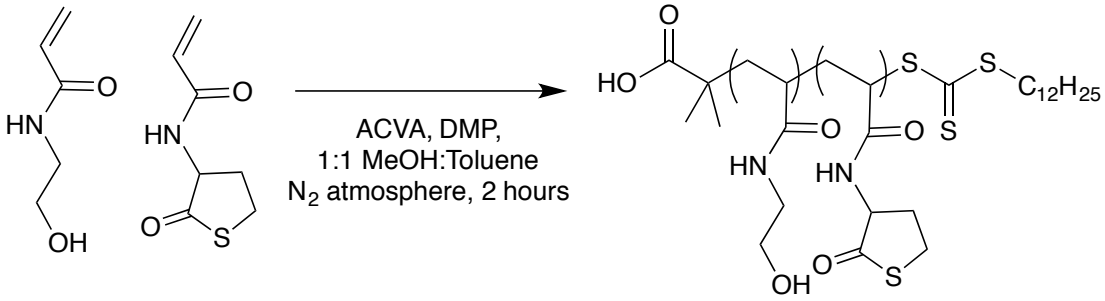

The following procedure describes a reaction with a theoretical degree of polymerisation (DP) of 50 repeat units, with 0.9 equivalents HEA and 0.1 equivalents TLa. 4,4-azobis(4-cyanovaleric acid) (2.5 mg, 0.0089 mmol), 2- (dodecylthiocarbonothioylthio)-2-methylpropanoic acid (CTA, 32 mg, 0.088 mmol), *N*-hydroxyethyl acrylamide (0.458 g, 3.98 mmol) and *N*-thiolactone acrylamide (69 mg, 0.44 mmol) were dissolved in 1:1 methanol: toluene (3 mL) in a glass vial with a stirrer bar. Mesitylene (100 µL) was added and a sample was removed for ^{1}H-NMR analysis in $CDCl_3$. The reaction mixture was degassed by N_2 for 30 minutes, sealed and placed in a 70°C oil bath. After 2 hours, the solution was opened to air and quenched in $N_{2(l)}$. The polymer (pHEA-co-pTLa) was precipitated three times from methanol into diethyl ether to give a light yellow solid. The characterization below is from a theoretical 20% TLa copolymer.

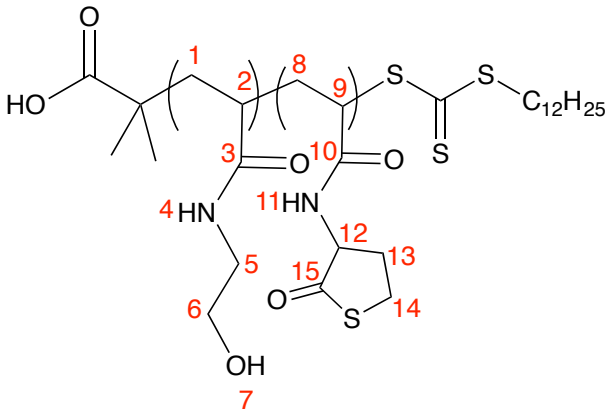

For 5% TLa: Conversion (NMR): 95.2%; Mn (theoretical): 4402 g.mol-1; Mn (SEC) 8585 g.mol-1; Mw (SEC) 9958 g.mol-1; Mw/Mn (SEC): 1.16. For 10% TLa: Conversion (NMR): 93.2%; Mn (theoretical): 4540 g.mol-1; Mn (SEC) 8912 g.mol-1; Mw (SEC) 10079 g.mol-1; Mw/Mn (SEC): 1.13.

^{1}H NMR (300 MHz, D4-MeOH) δppm: 7.9-8.15 (br s, N-H (H4/11)); 4.75-4.90 (br s, H6/14); 3.6-3.8 and 3.05-3.20 (2 x br s, H5/13); 2.55-2.7 (br s, H12 (this peak is less visible in 5 or 10% TLa copolymer)), 2.00-2.40 (the left should of this peak is less visible in 5 or 10% TLa copolymer) and 1.50-1.85 (2 x br m, H1/2/8/9).

FTIR (solid, νmax/cm-1) = 3300 (N-H and O-H stretch); 2854 (alkyl C-H stretch); 1641 (amide C=O stretch); 1555 (N-H bend); 1443 (alkane); 1225 (C-O stretch); 1060 (C-O stretch, peak has a shoulder); 920.

9.3.10 (Unsuccessful) General Procedure for Copolymerisation of *N*-isopropyl acrylamide (NIPAM) and *N*-thiolactone acrylamide (TLa)

The following procedure describes a reaction with a theoretical degree of polymerisation (DP) of 50 repeat units, with 0.9 equivalents NIPAM and 0.1 equivalents TLa. 4,4-azobis(4-cyanovaleric acid) (2.5 mg, 0.0089 mmol), 2- (dodecylthiocarbonothioylthio)-2-methylpropanoic acid (CTA, 16 mg, 0.044 mmol), N-isopropyl acrylamide (0.225 g, 7.96 mmol) and *N*-thiolactone acrylamide (32.5 mg, 0.884 mmol) were dissolved in 1:1 methanol: toluene (2 mL) in a glass vial with a stirrer bar. Mesitylene (100 µL) was added and a sample was removed for ^{1}H-NMR analysis in $CDCl_3$. The reaction mixture was degassed by N_2 for 30 minutes, sealed and placed in a 70°C oil bath. After 2 hours, the solution was opened to air and quenched in $N_{2(l)}$. The polymer (pNIPAM-co-pTLa) was precipitated three times from methanol into diethyl ether to give a light yellow solid. As this reaction was unsuccessful, no successful characterisation data is available.

9.3.11 General Procedure for Polymerisation of *N*-thiolactone acrylamide (TLa)

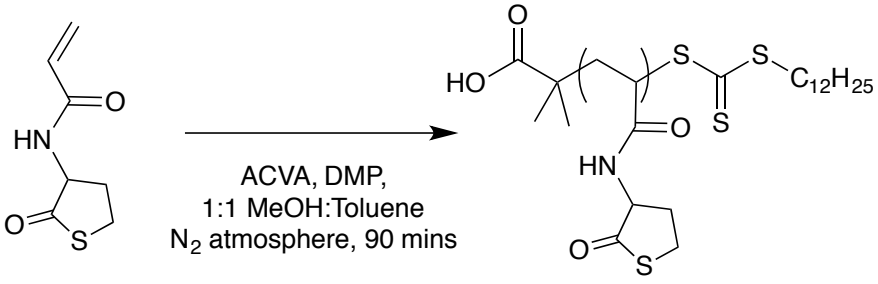

The following procedure describes a reaction with a theoretical degree of polymerisation (DP) of 50 repeat units. 4,4-azobis(4-cyanovaleric acid) (2.5 mg, 0.0089 mmol), 2-(dodecylthiocarbonothioylthio)-2-methylpropanoic acid (CTA, 16 mg, 0.044 mmol) and N-thiolactone acrylamide (0.325 g, 2.08 mmol) were dissolved in 1:1 methanol: toluene (2 mL) in a glass vial with a stirrer bar. Mesitylene (100 µL) was added and a sample was removed for ^{1}H-NMR analysis in $CDCl_3$. The reaction mixture was degassed by N_2 for 30 minutes, sealed and placed in a 70°C oil bath. After 45 minutes, the solution was opened to air and quenched in $N_{2(l)}$. The polymer (pTLa) was precipitated three times from chloroform into diethyl ether to give a light yellow solid.

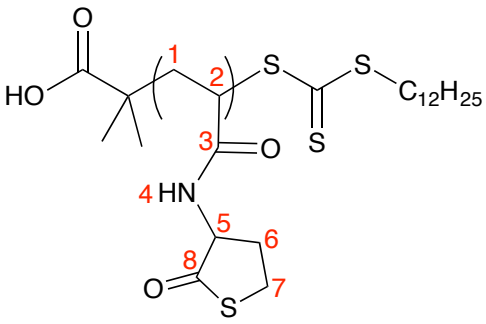

Conversion (NMR): 59.9%; M_n (theoretical): 3315 g.mol^{-1}; M_n (SEC) 5240g.mol^{-1}; M_w (SEC) 5835 g.mol^{-1}; M_w/M_n (SEC): 1.11.

^{1}H NMR (400 MHz, $CDCl_3$) δ_{ppm}: 7.0-7.25 (br s, N-H (H4)); 4.5-5.0 (br s, H7); 3.15-3.5 (br s, H6); 2.5-2.7 (br s, H5); 2.0-2.5 and 1.3-1.9 (2 x br m, H1/2).

FTIR (solid, ν_{max}/cm^{-1}) = 3330 (N-H); 2920 (CH_2); 1664 (C=O); 1570 (N-H); 1240 (C-N aliphatic); 1005 (=C-H bend); 920 (N-H wag).

9.3.12 Representative Double Modification of TLa-containing copolymer: Aminolysis and Thiol-ene "click"

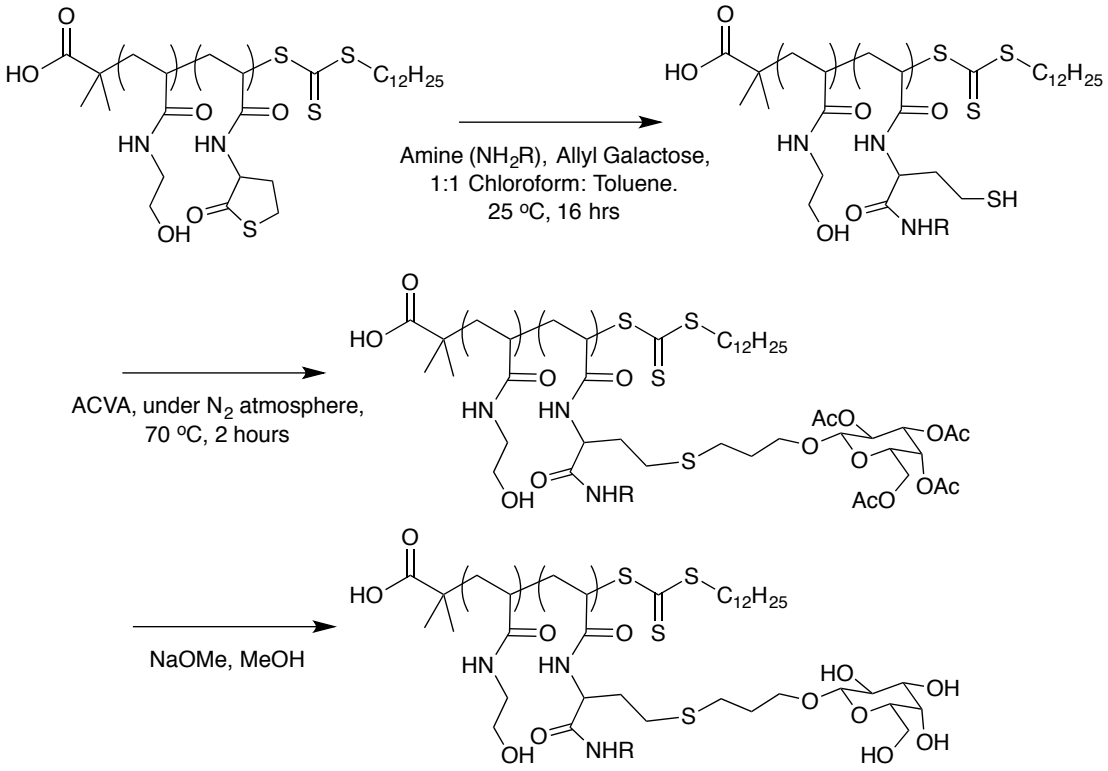

Polymer (100 mg of 5% pTLa copolymer) and amine (eg. 56 mg of glucosamine, 5 equivalents per TLa moiety) was dissolved in 1:1 methanol: water (5 mL) and stirred overnight at room temperature. Allyl galactose (67.4 mg, 5 equivalents per TLa moiety) and 4,4-azobis(4-cyanovaleric acid) (1.2 mg, 0.0045 mmol) were added. The reaction mixture was degassed by N_2 for 30 minutes, sealed and placed in a 70°C oil bath. After 2 hours, the solution was opened to air and quenched in $N_{2(l)}$. The reaction mixture was concentrated *in vacuo*, redissolved in methanol and filtered. The polymer was then precipitated three times from methanol into diethyl ether to give a light yellow solid. The different precipitation behaviour (all polymers were very difficult to dissolve in solution) was an indication of successful modification. The polymer was subsequently dissolved in methanol (5 mL) and deprotected with sodium methoxide (0.5 microL of 5.4 M solution in methanol) and precipitated three times from methanol into diethyl ether to give a light yellow solid.[40,77]

9.3.13 Representative Double Modification of TLa Homopolymer: Aminolysis and Thiol-ene "click"

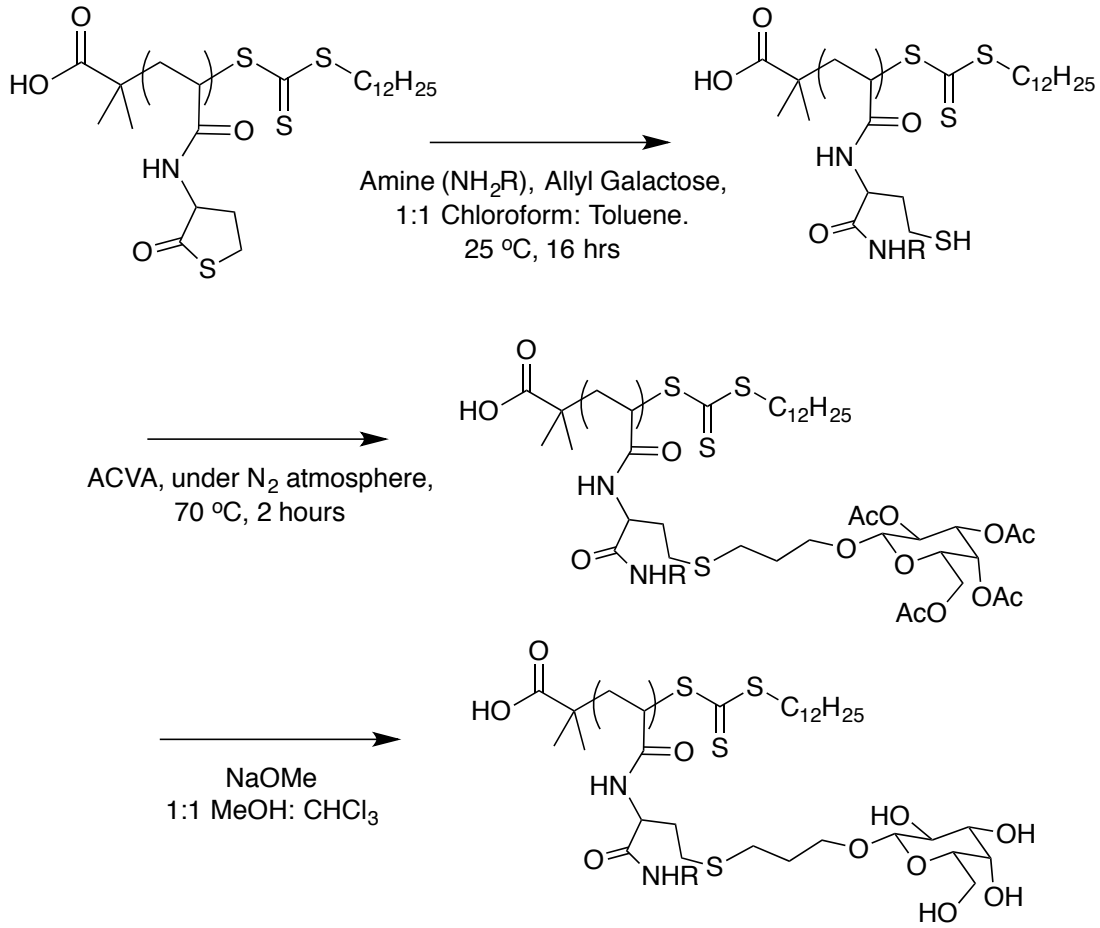

Polymer (80 mg) and amine (eg. 280 mg of glucosamine, 5 equivalents per TLa moiety) was dissolved in 1:1 chloroform: toluene (5 mL) and stirred overnight at room temperature. Allyl galactose (318 mg, 5 equivalents per TLa moiety) and 4,4-azobis(4-cyanovaleric acid) (5 mg, 0.017 mmol) were added. The reaction mixture was degassed by N_2 for 30 minutes, sealed and placed in a 70°C oil bath. After 2 hours, the solution was opened to air and quenched in $N_{2(l)}$. The reaction mixture was concentrated *in vacuo*, redissolved in chloroform and filtered. The polymer was then precipitated three times from 1:1 methanol: chloroform into diethyl ether to give a light yellow solid. The different precipitation behaviour (all polymers were very difficult to dissolve in solution) was an indication of successful modification. The polymer was subsequently dissolved in 1:1 methanol: chloroform (5 mL) and deprotected with sodium methoxide (1 microL of 5.4 M solution in methanol) and precipitated three times from 1:1 methanol: chloroform into diethyl ether to give a light yellow solid.[40,77]

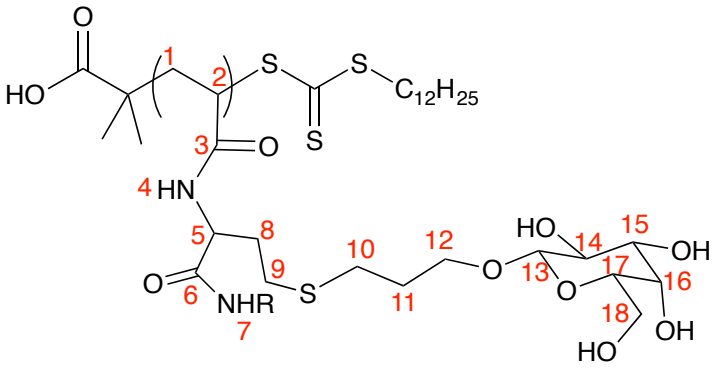

M_n (SEC) 8912 g.mol^{-1}; M_w (SEC) 10079 g.mol^{-1}; M_w/M_n (SEC): 1.13.

Protected polymer (did not perform deprotection step): ^{1}H NMR (400 MHz, $CDCl_3$) δ_{ppm}: 4.5-5.0 (br s, H7); 3.5-3.75 (2 x br m, very weak, possible sugar moieties); 3.15-3.5 (br s, H6); 2.5-2.7 (br s, H5); 2.0-2.2 (br strong s, acetyl groups); 2.0-2.5 and 1.3-1.9 (2 x br m, H1/2).

FTIR (solid, ν_{max}/cm^{-1}) = 3290 (N-H); 2900 (CH_2); 1655 (C=O); 1527 (N-H); 1055 (C-N aliphatic).

9.3.14 Fluorescence-linked sorbent assay for polymer inhibitory activity

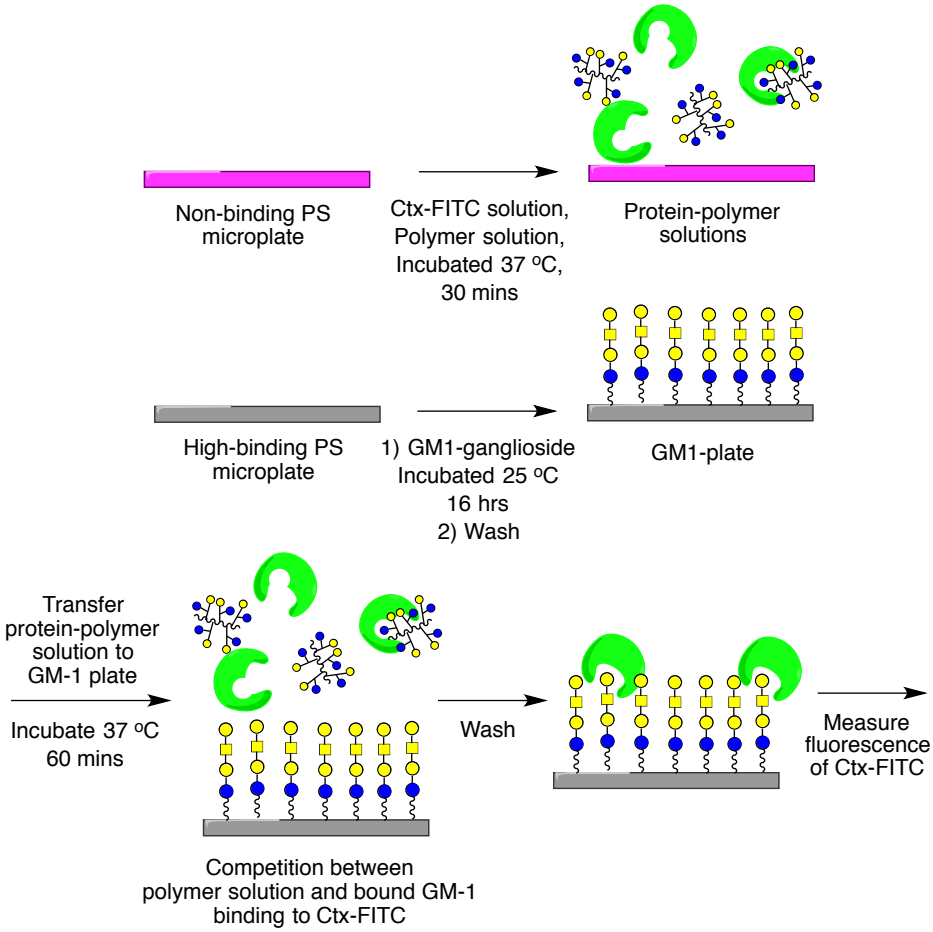

384-well high-binding PS plates were incubated for 16 hours with 50 µL of 100 µg.mL^{-1} GM-1 glycolipid (in PBS). Unbound glycolipid was removed by washing with water (x3). Polymer solutions were made up as serial dilutions (up to 12 dilutions by 2 from 1 mg.mL^{-1} in water; though 100% TLa polymers required initial dissolution in DMSO). CTx-FITC (4 µL of 100 µg.mL^{-1} in 10mM HEPES buffer with 0.15 M NaCl, 0.1 mM $CaCl_2$ and 0.01 mM Mn^{2+} (pH 7.5)) was added to 36 µL of polymer solution. The CTx/polymer solutions were then transferred to the GM-1-coated plates and incubated at 37°C for 60 minutes. The wells were then washed (x3) with HEPES buffer. Fluorescence of wells was measured at excitation/emission wavelengths of 485/528 nm respectively. All experiments were carried out in triplicate, using pure CTx-FITC wells (with no polymer) as controls. The above protocol is repeated for RCA-FITC to compare polymer inhibitory activity.

9.3.15 Synthesis of pentafluorophenyl 2-(dodecylthiocarbonothioylthio)-2-methylpropionic acid (PFP-DMP/PFP-DDMAT)

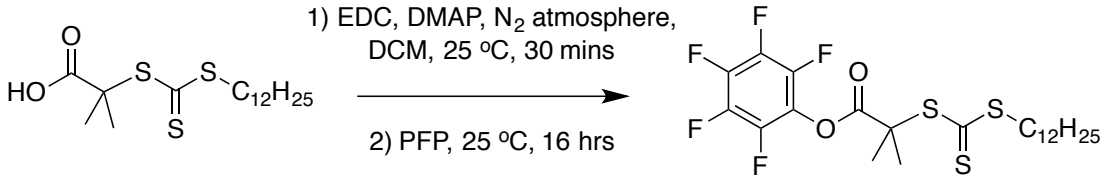

2-(Dodecylthiocarbonothioylthio)-2-methylpropionic acid (DMP) (0.500 g, 1.37 mmol), *N*-(3-dimethylaminopropyl)-*N*′-ethylcarbodiimide hydrochloride (EDC) (0.390 g, 2.05 mmol), and 4-(dimethylamino)pyridine (DMAP) (0.250 g, 2.05 mmol) were dissolved in DCM (50 mL) and stirred for 20 minutes under N_2. Pentafluorophenol (PFP) (0.780 g, 4.24 mmol) in 5 mL DCM was added. The reaction was stirred overnight at room temperature. The reaction was washed with 3 M HCl (100 mL), 1 M $NaHCO_3$ (100 mL) and brine (100 mL), dried over $MgSO_4$, filtered and then concentrated *in vacuo* to evolve a yellow solid with melting point close to room temperature (0.437 g, 60.2%).

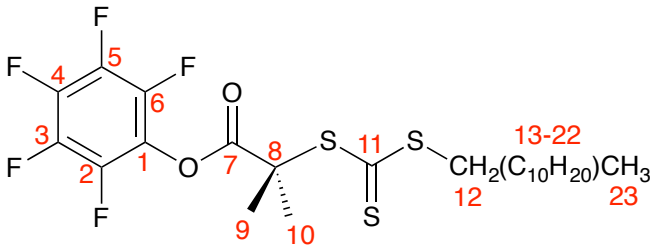

^{1}H NMR (300 MHz, CDCl3) δ_{ppm}: 3.24 (2H, t, J_{HH}=7.4 x 2, H12); 1.62 (6H, m, H9/10); 1.26 (20H, alkyl, H13-22); 0.81 (3H, m, H23).

^{19}F NMR (300 MHz, CDCl3) δ_{ppm}: 151.54 (m, F2/6), 157.74 (m, F3/5), 162.3 (m, F4).

FTIR (solid, ν_{max}/cm^{-1}): 2934 (CH_2); 1705 (C_6F_5C=O); 1439 (C-C); 1260 (C-O); 1080 (S-(C=S)-S).

9.3.16 General Procedure for Synthesis of PFP-pHEA polymer

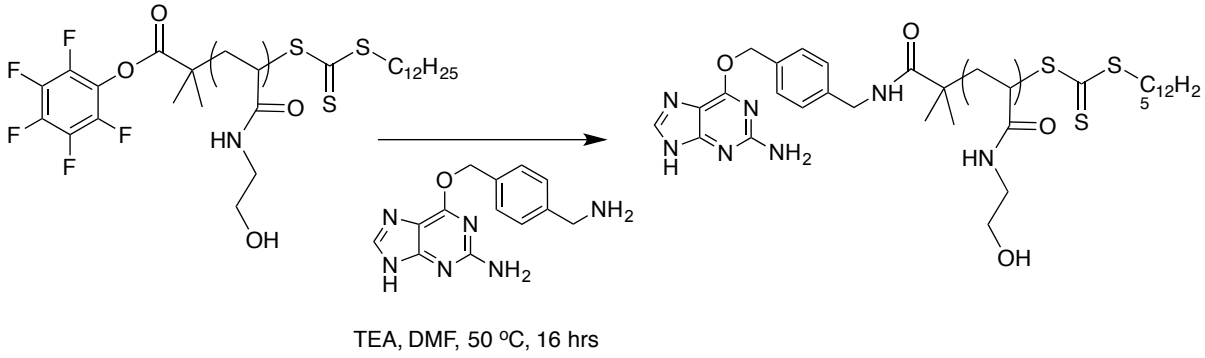

The following procedure describes a reaction with a theoretical degree of polymerisation (DP) of 50 repeat units. 4,4-azobis(4-cyanovaleric acid) (5 mg, 0.018 mmol), pentafluorophenyl 2-(dodecylthiocarbonothioylthio)-2-methylpropionic acid (CTA) (47 mg, 0.088 mmol) and *N*-hydroxyethyl acrylamide (1 g, 8.8 mmol) were dissolved in 1:1 methanol: toluene (4 mL) in a glass vial with a stirrer bar. Mesitylene (200 µL) was added and a sample was removed for ^{1}H-NMR analysis in $CDCl_3$. The reaction mixture was degassed by N_2 for 30 minutes, sealed and placed in a 70°C oil bath. After 90 minutes, the solution was opened to air and quenched in $N_{2(l)}$. The polymer (pHEA) was precipitated three times from methanol into diethyl ether to give a light yellow solid.

Conversion (NMR): 91.7%; Mn (theoretical): 5574 g.mol-1; Mn (SEC) 9264 g.mol-1; Mw (SEC) 10843 g.mol-1; Mw/Mn (SEC): 1.17.

^{1}H NMR (300 MHz, $CDCl_3$) δ_{ppm}: 8-8.15 (br s, N-H (H4)); 3.4-3.8 and 3.05-3.2 (2 x m, H5); 1.9-2.35 and 1.4-1.8 (2 x m, H1/2).

^{19}F NMR (300 MHz, $CDCl_3$) δ_{ppm}: 155.29, 161.61, 165.67.

FTIR (solid, ν_{max}/cm^{-1}) = 3300 (N-H and O-H stretch); 2854 (alkyl C-H stretch); 1641 (amide C=O stretch); 1555 (N-H bend); 1443 (alkane); 1225 (C-O stretch); 1060 (C-O stretch); 950 (C-F peak on shoulder of 1060 peak).

9.3.17 General Procedure for Synthesis of BG-pHEA polymer

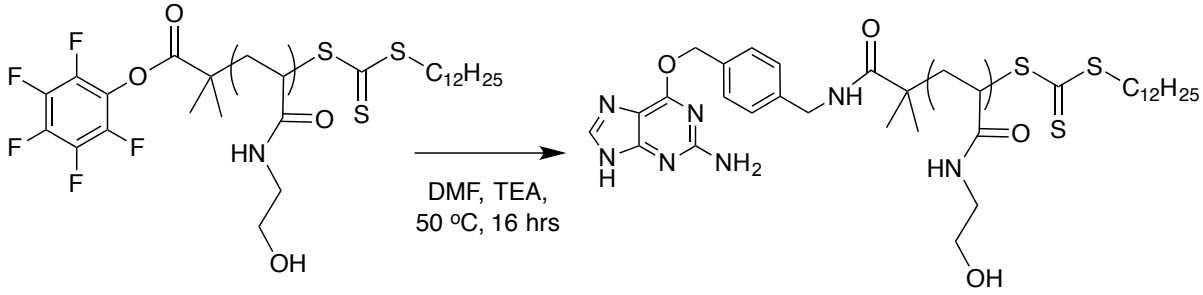

PFP-pHEA (90.8 mg, 0.018 mmol) and 6-((4-(aminomethyl)benzyl)oxy)-7H-purin-2-amine (23.8 mg, 0.088 mmol) were dissolved in DMF (5 mL). To the stirred mixture, triethylamine (35 µL) was added, and the reaction was moved to a 50 °C oil bath for 16 hours. The polymer (BG-pHEA) was precipitated three times from methanol into diethyl ether to give a sandy yellow solid.

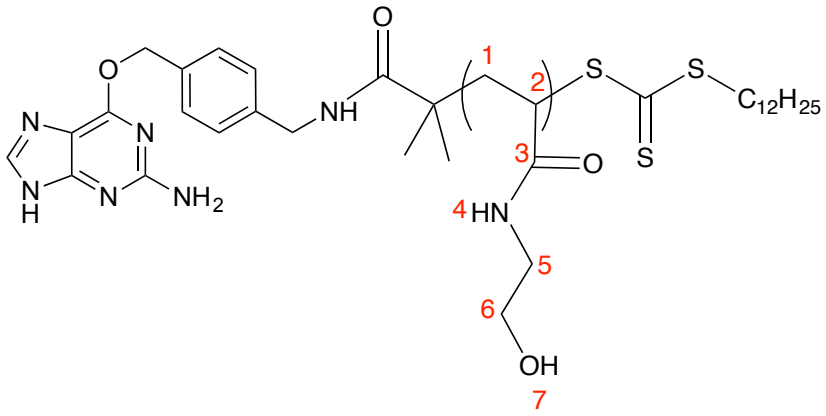

M_n (SEC) 12960 g.mol^{-1}; M_w (SEC) 15977 g.mol^{-1}; M_w/M_n (SEC): 1.23.

^{1}H NMR (300 MHz, D_4-MeOH) δ_{ppm}: 4.8-5 (br s, H6), 3.44-3.85 and 3.05-3.22 (2 x br s, H5), 1.94-2.35 and 1.31-1.86 (2 x br s, H1/2).

^{19}F NMR (300 MHz, $CDCl_3$) δ_{ppm}: no peaks visible.

FTIR (solid, ν_{max}/cm^{-1}) = 3300 (N-H and O-H stretch); 2854 (alkyl C-H stretch); 1641 (amide C=O stretch); 1555 (N-H bend); 1443 (C-H alkane); 1225 (C-O stretch); 1060 (C-O stretch) (C-F shoulder on 1060 peak is no longer present).

9.3.18 General Procedure for Synthesis Polymer-Coated Gold Nanoparticles (PFP-pHEA- or BG-pHEA-AuNPs)

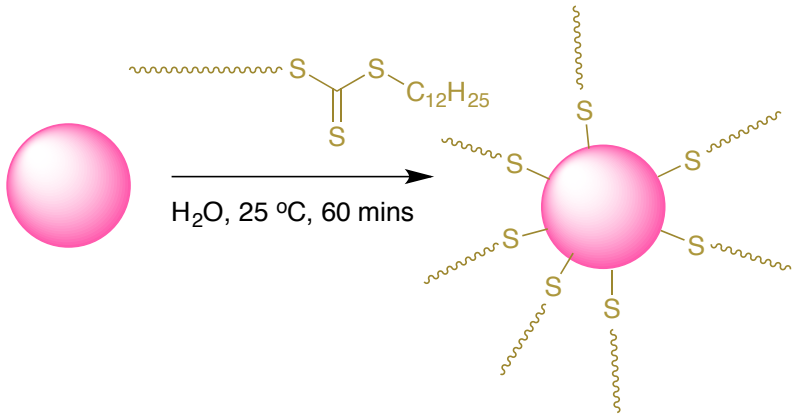

1 mg of polymer (either PFP-pHEA control polymers or BG-pHEA polymer) was added to 1 mL of gold nanoparticles (either 15 or 40 nm) in a 1.5 mL Eppendorf tube. This was left, covered with foil, for 60 minutes. The solution was centrifuged at 10,000 rpm, for 10 minutes, supernatant removed, and the pellet re- dispersed in 1 mL water. The nanoparticles were washed in this manner a further 3 times before being re-dispersed in a final volume of 1 mL distilled water and stored in the fridge until required.

9.3.19 Synthesis of 1-b-propargyl-D-galactose

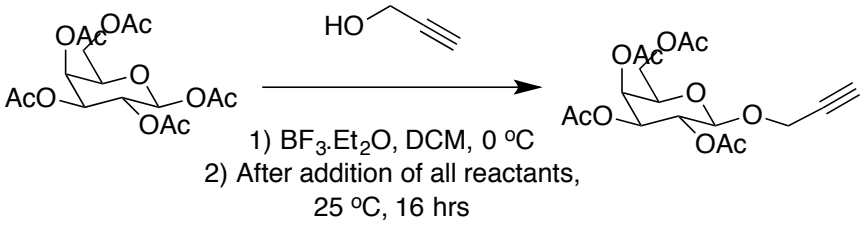

Beta-D-galactose pentaacetate (2.00 g, 5.13 mmol) was dissolved in DCM (40 mL). Propargyl alcohol (0.36 mL, 6.25 mmol) was added whilst stirring in an ice bath. Boron trifluoride diethetate (1.35 mL, 7.11 mmol) was added dropwise. 20 minutes later, the reaction was taken out of the ice bath and stirred for 16 hours. Anhydrous potassium carbonate (1.08 g, 7.24 mmol) was added whilst stirring. 30 minutes later, the reaction was filtered and washed with water (2 x 50 mL) and brine (50 mL). The organic layer was dried over $MgSO_4$, filtered and concentrated *in vacuo*. The residue was purified by column chromatography on silica using an eluent comprising 45:55 ethyl acetate: 40 – 60 ^{o}C petroleum ether to yield a sticky, viscous yellow oil (0.420 g, 21.1% - note that this yield is low due to loss of product during successive unsuccessful recrystallization attempts)

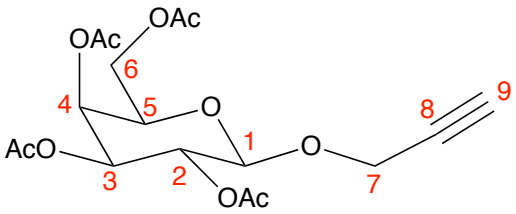

^{1}H NMR (400 MHz, $CDCl_3$) δ_{ppm}: 5.43 (1H, m, H1); 5.24 (1H, m, H4); 5.09 (1H, m, H2); 4.75 (1H, m, H7); 4.4 (2H, d, J_{HH}=2.3, H6); 4.17 (1H, m, H3); 3.96 (1H, m, H5); 2.49 (1H, m, H9); 2.19, 2.09, 2.07, 2.01 (15H, 4 x s, acetyl groups)

^{13}C NMR (400 MHz, $CDCl_3$) δ_{ppm}: 99.86 (CH, C9), 75.36 (CH_2, C7), 70.83 (CH, C1/4), 68.50 (CH, C2), 66.98 (CH, C3), 61.20 (CH_2, C6), 55.90 (C, C8), 30.93 (CH, C5), 20-21 (CH_3, Acetyls).

FTIR (solid, ν_{max}/cm^{-1}): 3274 (O-H); 2941 (CH_2); 1739 (C=O); 1368 (C-H); 1212 (C-O stretch).

ESI-MS, positive mode (m/z): 409.1 ($M+Na^+$, expected 409.34).

9.3.20 (Unsuccessful) Azide-modification of Poly(3-hexylthiophene-2,5-diyl)-Br (P3HT-Br) with Sodium Azide

P3HT (50 mg, 0.0138 mmol) was dissolved in toluene (60 mL). Sodium azide (0.0181g, 0.278 mmol) in methanol (10 mL) was added. A condenser was attached above the reaction vessel, and the reaction was stirred reflux overnight. The polymer (P3HT-N_3) was precipitated three times from toluene into methanol to give a dark red solid. This reaction was unsuccessful most likely due to the solubility of

sodium azide in protic solvents only, and P3HT's solubility in only toluene or THF – meaning that the azide likely precipitated out during the reaction without acting on the bromide.

9.3.21 Azide-modification of Poly(3-hexylthiophene-2,5-diyl)-Br (P3HT-Br)

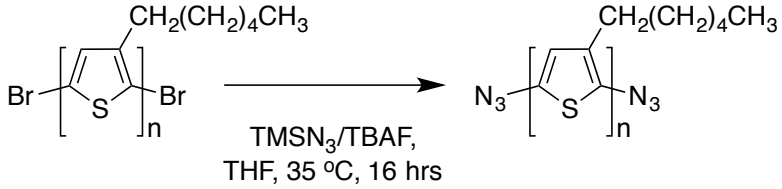

P3HT (20 mg, 0.0055 mmol) was dissolved in THF (60 mL). Trimethylsilyl azide (3 µL, 0.0228 mmol) and tetrabutylammonium fluoride (22.7 µL of 1.0 M solution in THF, 0.0228 mmol) were added whilst stirring. An air condenser was attached above the reaction vessel, and the reaction was stirred at 35°C overnight. The polymer (P3HT-N_3) was precipitated three times from THF into ethanol to give a dark red solid.

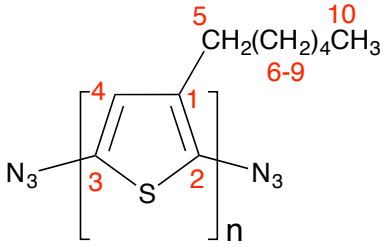

1H NMR (300 MHz, CDCl3) δppm: 7.07 (m, H4), 2.87 (m, H5), 1.69 (m, H6), 1.31 (H7-9), 0.95 (H10).

FTIR (solid, ν_{max}/cm^{-1}): 2920 (CH_2); 1450 (C-C aromatic stretch); 1380, 1260 (both C-H); 880 (C-H "oop"); 730 (C-H rock) – note that a peak at 660 (indicative of C-Br) is not present in the product.

10 Bibliography

(1) Ratner, B. D., and Bryant, S. J. (2004) Biomaterials: Where We Have Been and Where We Are Going. *Rev. Lit. Arts Am.* 41–75.

(2) Langer, R., and Tirrell, D. a. (2004) Designing materials for biology and medicine. *Nature 428*, 487–492.

(3) Richards, S.-J., Fullam, E., Besra, G. S., and Gibson, M. I. (2014) Discrimination between bacterial phenotypes using glyco-nanoparticles and the impact of polymer coating on detection readouts. *J. Mater. Chem. B 2*, 1490–1498.

(4) Pache, C., Bocchio, N. L., Bouwens, A., Villiger, M., Berclaz, C., Goulley, J., Gibson, M. I., Santschi, C., and Lasser, T. (2012) Fast three-dimensional imaging of gold nanoparticles in living cells with photothermal optical lock-in Optical Coherence Microscopy. *Opt. Express 20*, 21385.

(5) Richards, S. J., Jones, M. W., Hunaban, M., Haddleton, D. M., and Gibson, M. I. (2012) Probing bacterial-toxin inhibition with synthetic glycopolymers prepared by tandem post-polymerization modification: Role of linker length and carbohydrate density. *Angew. Chemie - Int. Ed. 51*, 7812–7816.

(6) Jones, M. W., Otten, L., Richards, S.-J., Lowery, R., Phillips, D. J., Haddleton, D. M., and Gibson, M. I. (2014) Glycopolymers with secondary binding motifs mimic glycan branching and display bacterial lectin selectivity in addition to affinity. *Chem. Sci. 5*, 1611.

(7) Gabius, H. J., Siebert, H. C., André, S., Jiménez-Barbero, J., and Rüdiger, H. (2004) Chemical biology of the sugar code. *ChemBioChem 5*, 740–764.

(8) Hudson, K. L., Bartlett, G. J., Diehl, R. C., Agirre, J., Gallagher, T., Kiessling, L. L., and Woolfson, D. N. (2015) Carbohydrate-Aromatic Interactions in Proteins. *J. Am. Chem. Soc. 137*, 15152–15160.

(9) Gaiano, N., and Fishell, G. (2004) Role of Glycosylation in Development. *Annu. Rev. Biochem. 73*, 491–537.

(10) Ohtsubo, K., and Marth, J. D. (2006) Glycosylation in Cellular Mechanisms of Health and Disease. *Cell 126*, 855–867.

(11) Bernardi, A., Jiménez-Barbero, J., Casnati, A., De Castro, C., Darbre, T., Fieschi, F., Finne, J., Funken, H., Jaeger, K.-E., Lahmann, M., Lindhorst, T. K., Marradi, M., Messner, P., Molinaro, A., Murphy, P. V, Nativi, C., Oscarson, S., Penadés, S., Peri, F., Pieters, R. J., Renaudet, O., Reymond, J.-L., Richichi, B., Rojo, J., Sansone, F., Schäffer, C., Turnbull, W. B., Velasco-Torrijos, T., Vidal, S., Vincent, S., Wennekes, T., Zuilhof, H., and Imberty, A. (2013) Multivalent glycoconjugates as anti-pathogenic agents. *Chem. Soc. Rev. 42*, 4709–4727.

(12) Varki, A. (2007) Glycan-based interactions involving vertebrate sialic-acid-recognizing proteins. *Nature 446*, 1023–9.

(13) Crater, W., Hadida, A., Chao, A. E. C. T., Fahey, J. J., Littler, J., and Walker, J. M. (1976) Surface Modulation in Cell Recognition and Cell Growth. *Science (80-.). 192*, 218–226.

(14) Lis, H., and Sharon, N. (1998) Lectins: Carbohydrate-Specific Proteins That Mediate Cellular Recognition. *Chem. Rev. (Washington, DC, United States) 98*, 637–674.

(15) Sharon, N. (2006) Carbohydrates as future anti-adhesion drugs for infectious diseases. *Biochim. Biophys. Acta - Gen. Subj. 1760*, 527–537.

(16) Bovin, N. V., Tuzikov, A. B., Chinarev, A. a., and Gambaryan, A. S. (2004) Multimeric glycotherapeutics: New paradigm. *Glycoconj. J. 21*, 471–478.

(17) Tran, H.-A., Kitov, P. I., Paszkiewicz, E., Sadowska, J. M., and Bundle, D. R. (2011) Multifunctional multivalency: a focused library of polymeric cholera toxin antagonists. *Org. Biomol. Chem. 9*, 3658–3671.

(18) Lundquist, J. J., and Toone, E. J. (2002) The cluster glycoside effect. *Chem. Rev. 102*, 555–578.

(19) Becer, C. R., Gibson, M. I., Geng, J., Ilyas, R., Wallis, R., Mitchell, D. a., and Haddleton, D. M. (2010) High-affinity glycopolymer binding to human DC-SIGN and disruption of DC-SIGN interactions with HIV envelope glycoprotein. *J. Am. Chem. Soc. 132*, 15130–15132.

(20) Kaper, J. B., Morris, J. G., and Levine, M. M. (1995) Cholera. *Clin. Microbiol. Rev. 8*, 48–86.

(21) Spangler, B. (1992) Structure and function of cholera toxin and the related Escherichia coli heat-labile enterotoxin. *Microbiol. Rev. 56*, 622–647.

(22) Holmgren, J., and Svennerholm, A. (2016) Mechanisms of Disease and Immunity in Cholera : A Review. *J. Infect. Dis. 136*.

(23) Holmgren, J., Lonnroth, I., and Svennerholm, L. (1973) Tissue receptor for cholera exotoxin: postulated structure from studies with G(M1) Ganglioside and related glycolipids. *Infect. Immun. 8*, 208–214.

(24) Braunecker, W. a., and Matyjaszewski, K. (2007) Controlled/living radical polymerization: Features, developments, and perspectives. *Prog. Polym. Sci. 32*, 93–146.

(25) Bajpai, a. K., Bajpai, J., Saini, R., and Gupta, R. (2011) Responsive Polymers in Biology and Technology. *Polym. Rev. 51*, 53–97.

(26) Lowe, A. B., and McCormick, C. L. (2007) Reversible addition-fragmentation chain transfer (RAFT) radical polymerization and the synthesis of water-soluble (co)polymers under homogeneous conditions in organic and aqueous media. *Prog. Polym. Sci. 32*, 283–351.

(27) Perrier, S., and Takolpuckdee, P. (2005) Macromolecular design via reversible addition-fragmentation chain transfer (RAFT)/xanthates (MADIX) polymerization. *J. Polym. Sci. Part A Polym. Chem. 43*, 5347–5393.

(28) An, Z., Qiu, Q., and Liu, G. (2011) Synthesis of architecturally well-defined nanogels via RAFT polymerization for potential bioapplications. *Chem. Commun. (Camb). 47*, 12424–40.

(29) Moad, G., Rizzardo, E., and Thang, S. H. (2008) Radical addition-fragmentation chemistry in polymer synthesis. *Polymer (Guildf). 49*, 1079–1131.

(30) Wilkins, L. E., Phillips, D. J., Deller, R. C., Davies, G. L., and Gibson, M. I. (2015) Synthesis and characterisation of glucose-functional glycopolymers and gold nanoparticles: Study of their potential interactions with ovine red blood cells. *Carbohydr. Res. 405*, 47–54.

(31) Skey, J., and O'Reilly, R. K. (2008) Facile one pot synthesis of a range of reversible addition-fragmentation chain transfer (RAFT) agents. *Chem. Commun.* 4183–4185.

(32) Meldal, M., and Tom??e, C. W. (2008) Cu-catalyzed azide - Alkyne cycloaddition. *Chem. Rev. 108*, 2952–3015.

(33) Slavin, S., Burns, J., Haddleton, D. M., and Becer, C. R. (2011) Synthesis of

glycopolymers via click reactions. *Eur. Polym. J. 47*, 435–446.

(34) Huisgen, R. (1968) Cycloadditions — Definition, Classification, and Characterization. *Angew. Chemie Int. Ed. English 7*, 321–328.

(35) Kolb, H. C., Finn, M. G., and Sharpless, K. B. (2001) Click Chemistry: Diverse Chemical Function from a Few Good Reactions. *Angew. Chemie - Int. Ed. 40*, 2004–2021.

(36) Liang, L., and Astruc, D. (2011) The copper(I)-catalyzed alkyne-azide cycloaddition (CuAAC) "click" reaction and its applications. An overview. *Coord. Chem. Rev. 255*, 2933–2945.

(37) Willcock, H., and O'Reilly, R. K. (2010) End group removal and modification of RAFT polymers. *Polym. Chem. 1*, 149–157.

(38) Gauthier, M., Gibson, M., and Klok, H.-A. (2009) Synthesis of Functional Polymers by Post-Polymerization Modification. *Angew. Chemie Int. Ed. 48*, 48–58.

(39) Günay, K. A., Theato, P., and Klok, H. A. (2013) History of Post-Polymerization Modification. *Funct. Polym. by Post-Polymerization Modif. Concepts, Guidel. Appl.* 1–44.

(40) Reinicke, S., Espeel, P., Stamenović, M. M., and Du Prez, F. E. (2013) One-pot double modification of p(NIPAAm): A tool for designing tailor-made multiresponsive polymers. *ACS Macro Lett. 2*, 539–543.

(41) Goethals, F., Martens, S., Espeel, P., Van Den Berg, O., and Du Prez, F. E. (2014) Diversely substituted polyamide structures through thiol-ene polymerization of renewable thiolactone building blocks. *Macromolecules 47*, 61–69.

(42) Espeel, P., Goethals, F., and Du Prez, F. E. (2011) One-pot multistep reactions based on thiolactones: Extending the realm of thiol-ene chemistry in polymer synthesis. *J. Am. Chem. Soc. 133*, 1678–1681.

(43) Rudolph, T., Espeel, P., Du Prez, F. E., and Schacher, F. H. (2015) Poly(thiolactone) homo- and copolymers from maleimide thiolactone: synthesis and functionalization. *Polym. Chem. 6*, 4240–4251.

(44) Zhao, Y., Yang, B., Zhang, Y., Wang, S., Fu, C., Wei, Y., and Tao, L. (2014) Fluorescent PEGylation agent by a thiolactone-based one-pot reaction: A new strategy for theranostic combinations. *Polym. Chem. 5*, 6656–6661.

(45) Reinicke, S., Espeel, P., Stamenović, M. M., and Du Prez, F. E. (2014) Synthesis of multi-functionalized hydrogels by a thiolactone-based synthetic protocol. *Polym. Chem. 5*, 5461.

(46) Belbekhouche, S., Reinicke, S., Espeel, P., Du Prez, F. E., Eloy, P., Dupont-Gillain, C., Jonas, A. M., Demoustier-Champagne, S., and Glinel, K. (2014) Polythiolactone-based redox-responsive layers for the reversible release of functional molecules. *ACS Appl. Mater. Interfaces 6*, 22457–22466.

(47) Espeel, P., and Du Prez, F. E. (2015) One-pot multi-step reactions based on thiolactone chemistry: A powerful synthetic tool in polymer science. *Eur. Polym. J. 62*, 247–272.

(48) Stamenović, M. M., Espeel, P., Baba, E., Yamamoto, T., Tezuka, Y., and Du Prez, F. (2012) Straightforward synthesis of functionalized cyclic polymers in high yield via RAFT and thiolactone/disulfide chemistry. *Polym. Chem. 4*, 184–193.

(49) Espeel, P., Goethals, F., Stamenović, M. M., Petton, L., and Du Prez, F. E. (2012) Double modular modification of thiolactone-containing polymers: towards polythiols and derived structures. *Polym. Chem. 3*, 1007.

(50) Thadke, S. A., Kar, M., Gupta, S. Sen, and Hotha, S. (2011) Gold catalyzed glycosidations for the synthesis of sugar acrylate/acrylamide hybrids and their utility. *Carbohydr. Res. 346*, 1511–1518.

(51) Agyei-Aye, K., Chian, M. X., Lauterbach, J. H., and Moldoveanu, S. C. (2002) The role of the anion in the reaction of reducing sugars with ammonium salts. *Carbohydr. Res. 337*, 2273–2277.

(52) Meinjohanns, E., Meldal, M., Paulsen, H., A. Dwek, R., and Bock, K. (1998) Novel sequential solid-phase synthesis of N-linked glycopeptides from natural sources. *J. Chem. Soc. Perkin Trans 1 1*, 549–560.

(53) Smits, E., Engberts, J. B. F. N., Kellog, R. M., and van Doren, H. A. (1996) Reliable method for the synthesis of aryl beta-d-glucopyranosides, using boron trifluoride-diethyl ether as a catalyst. *J. Chem. Soc. Perkin Trans. 1* 2873–2877.

(54) Gibson, M. I., Danial, M., and Klok, H. A. (2011) Sequentially modified, polymer-stabilized gold nanoparticle libraries: Convergent synthesis and aggregation behavior. *ACS Comb. Sci. 13*, 286–297.

(55) Sun, X., Zhang, A., Baker, B., Sun, L., Howard, A., Buswell, J., Maurel, D., Masharina, A., Johnsson, K., Noren, C. J., Xu, M. Q., and Corrêa, I. R. (2011) Development of SNAP-tag fluorogenic probes for wash-free fluorescence imaging. *ChemBioChem 12*, 2217–2226.

(56) Dreier, B., and Plückthun, A. (2012) Ribosome Display and Related Technologies. *Methods Mol. Biol. 805*, 261–286.

(57) Mottram, L. F., Maddox, E., Schwab, M., Beaufils, F., and Peterson, B. R. (2007) A concise synthesis of the pennsylvania green fluorophore and labeling of intracellular targets with O 6-benzylguanine derivatives. *Org. Lett. 9*, 3741–3744.

(58) Hussain, A. F., Kampmeier, F., Von Felbert, V., Merk, H. F., Tur, M. K., and Barth, S. (2011) SNAP-tag technology mediates site specific conjugation of antibody fragments with a photosensitizer and improves target specific phototoxicity in tumor cells. *Bioconjug. Chem. 22*, 2487–2495.

(59) Shi, G., Azoulay, M., Dingli, F., Lamaze, C., Loew, D., Florent, J. C., and Johannes, L. (2012) SNAP-tag Based Proteomics Approach for the Study of the Retrograde Route. *Traffic 13*, 914–925.

(60) Cole, N. B., and Donaldson, J. G. (2012) Releasable SNAP-tag probes for studying endocytosis and recycling. *ACS Chem. Biol. 7*, 464–469.

(61) Campos, C., Kamiya, M., Banala, S., Johnsson, K., and Gonz??lez-Gait??n, M. (2011) Labelling cell structures and tracking cell lineage in zebrafish using SNAP-tag. *Dev. Dyn. 240*, 820–827.

(62) Waterfield, N. R., Ciche, T., and Clarke, D. (2009) Photorhabdus and a host of hosts. *Annu. Rev. Microbiol. 63*, 557–74.

(63) Yin, J., Zhu, H., Xia, L., Ding, X., Hoffmann, T., Hoffmann, M., Bian, X., M??ller, R., Fu, J., Stewart, a. F., and Zhang, Y. (2015) A new recombineering system for Photorhabdus and Xenorhabdus. *Nucleic Acids Res. 43*, e36.

(64) Brachmann, A. O., Kirchner, F., Kegler, C., Kinski, S. C., Schmitt, I., and Bode, H. B. (2012) Triggering the production of the cryptic blue pigment indigoidine from Photorhabdus luminescens. *J. Biotechnol. 157*, 96–99.

(65) Yang, G., Dowling, a. J., Gerike, U., Ffrench-Constant, R. H., and Waterfield, N. R. (2006) Photorhabdus virulence cassettes confer injectable insecticidal activity against the wax

moth. *J. Bacteriol. 188*, 2254–2261.

(66) Lee, E. S., Kim, D., Youn, Y. S., Oh, K. T., and Bae, Y. H. (2008) A virus-mimetic nanogel vehicle. *Angew. Chemie - Int. Ed. 47*, 2418–2421.

(67) Otten, L., Vlachou, D., Richards, S.-J., and Gibson, M. I. (2016) Glycan Heterogeneity On Gold Nanoparticles Increases Lectin Discrimination Capacity in Label-Free Multiplexed Bioassays. *Analyst*.

(68) Li, Y. (2012) Molecular design of photovoltaic materials for polymer solar cells: Toward suitable electronic energy levels and broad absorption. *Acc. Chem. Res. 45*, 723–733.

(69) Kroon, R., Lenes, M., Hummelen, J. C., Blom, P. W. M., and de Boer, B. (2008) Small Bandgap Polymers for Organic Solar Cells (Polymer Material Development in the Last 5 Years). *Polym. Rev.*

(70) Kolomanska, J., Johnston, P., Gregori, A., Dominguez, I. F., Egelhaaf, H.-J., Perrier, S., Rivaton, A., Dagron-Lartigau, C., and Topham, P. D. (2015) Design, synthesis and thermal behaviour of a series of well-defined clickable and triggerable sulfonate polymers. *Rsc Adv. 5*, 66554–66562.

(71) Monnaie, F., Brullot, W., Verbiest, T., De Winter, J., Gerbaux, P., Smeets, A., and Koeckelberghs, G. (2013) Synthesis of end-group functionalized P3HT: General protocol for P3HT/nanoparticle hybrids. *Macromolecules 46*, 8500–8508.

(72) Topham, P. D., Parnell, A. J., and Hiorns, R. C. (2011) Block copolymer strategies for solar cell technology. *J. Polym. Sci. Part B Polym. Phys. 49*, 1131–1156.

(73) Haase, J. (2010) Large-Scale Preparation and Usage of Azides. *Org. Azides Synth. Appl.*

(74) Soli, E. D., Manoso, A. S., Patterson, M. C., DeShong, P., Favor, D. A., Hirschmann, R., and Smith, A. B. (1999) Azide and cyanide displacements via hypervalent silicate intermediates. *J. Org. Chem. 64*, 3171–3177.

(75) De Winter, J., Deshayes, G., Boon, F., Coulembier, O., Dubois, P., and Gerbaux, P. (2011) MALDI-ToF analysis of polythiophene: Use of trans-2-[3-(4-t-butyl-phenyl)- 2-methyl-2-propenylidene]malononitrile - DCTB - as matrix. *J. Mass Spectrom. 46*, 237–246.

(76) Sciences, L., and All, A. (1999) Opposite effects of D-glucose pentaacetate and D-galactose pentaacetate anomers on insulin release evoked by succinic acid dimethyl ester in rat pancreatic islets. *Life Sci. 64*, 751–754.

(77) Sardzik, R., Sharma, R., Kaloo, S., Voglmeir, J., Crocker, P. R., and Flitsch, S. L. (2011) Chemoenzymatic synthesis of sialooligosaccharides on arrays for studies of cell surface adhesion. *Chem. Commun. 47*, 5425–5427.